Daniel Augusto Santos

Modelos cranianos 3D: nova abordagem craniométrica

3D skull models: a new craniometric approach

**Daniel Augusto
Santos**

**Modelos cranianos 3D: nova abordagem
craniométrica**

3D skull models: a new craniometric approach

“*He who would learn to fly one day must first learn to walk and
run and climb and dance; one cannot fly into flying.*”

— Friedrich Wilhelm Nietzsche

**Daniel Augusto
Santos**

**Modelos cranianos 3D: nova abordagem
craniométrica**

3D skull models: a new craniometric approach

Dedico este trabalho à minha falecida avó, Amélia da Conceição.

o júri / the jury

presidente / president

Prof. Doutor José Manuel Matos Moreira
Professor Auxiliar da Universidade de Aveiro

vogais / examiners committee

Prof. Doutor Jaime dos Santos Cardoso
Professor Auxiliar da Faculdade de Engenharia da Universidade do Porto

Prof. Doutor Paulo Miguel de Jesus Dias
Professor Auxiliar do Departamento de Eletrónica, Telecominicações e Informática da Universidade de Aveiro

Prof. Doutora Maria Beatriz Alves de Sousa Santos
Professora Associada c/ Agregação do Departamento de Eletrónica, Telecominicações e Informática da Universidade de Aveiro

agradecimentos /
acknowledgements

Palavras Chave   Craniometria, Modelos 3D, Aquisição 3D

Resumo   Esta dissertação apresenta uma nova abordagem para realizar análises craniométricas com base em modelos 3D de crânios. Atualmente o procedimento usado pelos antropólogos assenta no recurso a craniometria tradicional, i.e. medições manuais, o que implica variados problemas tais como dificuldade em assegurar repetibilidade das medições, erros na mesmas e possível dano nos crânios inerente ao seu manuseamento. A abordagem proposta passa por fazer a aquisição dos crânios recorrendo a um scanner 3D de luz estruturada (realizada por terceiros) e posterior análise recorrendo a uma aplicação especificamente desenvolvida para tal, e na qual assenta o trabalho descrito neste documento. Vários métodos serão abordados, tais como análise de malhas 3D, estudos de normais e curvaturas, obtenção de pontos de interesse e respectivas medidas e, por fim, serão apresentadas conclusões sobre o trabalho, bem como sugestões de trabalho futuro.

Abstract   This dissertation presents a new approach to conduct craniometric analysis
based on 3D models of skulls. Nowadays procedures used by anthropologists
are based in traditional methods, i.e. manual measurements, which may imply
a set of problems such as difficulty in ensuring repeatability of the measure-
ments, measurement errors and can skull damage inherent to the handling.
The new approach lies on the acquisition of the skulls using a structured 3D
light scanner (done by a third party entity) and subsequent analysis using an
application specifically designed for that purpose. Is on the latter that this work
is based. Several methods are going to be addressed, such as analysis of 3D
meshes, studies of normal vectors and curvatures, obtainment of points of
interest (landmark points) and measurements. Finally, conclusions about the
developed methods, results and future work.

Contents

List of Figures

List of Tables

Introduction

THIS dissertation is a collaboration between IEETA[1], the company Dryas Archaeology[2], and CENCIFOR[3]. It presents a new approach to perform craniometric analysis from digital models, resulting of the acquisition process with a 3D structured light scanning system, instead of direct manipulation of the original skulls. The document will describe the researched and developed methods and tools on the subject and, as well, the obtained results and conclusions.

Craniometric analysis is the main tool used in Anthropology to identify gender, ancestry and variations in populations [1]. The determination of these characteristics is typically performed using traditional craniometric measurements (physically measured in the skulls)[2], [3]. These traditional techniques suffer from several drawbacks: poor repeatability (intra- and inter-observer errors), impossibility to perform on fragments and/or in fragmented skulls, inadequacy to describe complex shapes and the need for actual contact with the skulls that may damage the bones. The question of bones damage is of crucial importance since, once the damage is done, some information may have been lost forever and, consequently, the opportunity to use the data to discover something relevant.

The main objective of this thesis was the development of *(software)* tools to make possible, from the acquired 3D models, the calculation of the principal craniometric measures used by anthropologists to caracterize the skulls.
The initially defined objectives were following:

1. Study of the relevant topics in the craniometry science and work already done on this field.

---

2. Development of *software* tools to obtain craniometric measures *automatically/semi automatically/manually.*

3. Comparison (and validation) of the obtained results with the ones obtained from the traditionally used (manual) methods.

1.1 Motivation and Objectives

1.1.1 Craniometry

THE applicability of craniometry to anthropological research, as a diagnostic tool for gender and ancestry estimation, and human evolution studies is well known [2], [4]–[7]. The roots of anthropometry are traced back to the measurement of the skull by early scientists [2]. Simply defined, craniometry refers to the study of human cranial measurements for use in anthropological classification and comparison [2].

The protocol for gender and ancestry estimation by visual assessment of non metric traits typically involves the extraction of each feature of the skull and then sorting them into categories previously defined based on shape and size differences [2], [6], [8]–[10]. However, such approach has been largely criticized for being highly subjective [7]–[12]. Citing Hefner [8]: "The experience based method of ancestry prediction using morphoscopic traits indeed is an art: an art that is intuitive, untestable, unempirical, and consequently unscientific. It is often more appropriate to perform a metric analysis when working with morphological data, since it has proven to be more objective". Because measurements rely on standard landmarks, results exhibit lower levels of intra- and inter- observer errors [2], [9], [10]. Similarly there are more powerful statistical methods for the analysis of continuous data. Linear measurements are commonly evaluated by uni- and multivariate statistical analysis, like discriminant functions [2], [6], [13], [14]. Nevertheless, traditional linear measurements are not able to capture the shape differences of some complex and rounded structures, e.g. orbit shape [7], [12]. Because of that, with a greater emphasis put on shape rather than size, visual assessment methodologies provided the most appreciated way to assess shape differences, at least until recently [2], [9], [10], [12]. A major change started at the ending of last century. Data regarding the geometry of the morphological structure employing 3D coordinates of anatomical landmarks were of particular interest, and methods to analyze such data started to be developed [6], [7], [9], [10], [15]. This approach offers some advantages in relation to linear measurements. Investigators can preserve geometric information about the relative positions of coordinated points, visualize results of multivariate analyses as configurations of landmarks back in the original space of the organism, and assess variation in structures with few or no landmarks

[5]–[7], [9], [10]. Thus, geometric morphometrics would be more appropriate to describe differences in structures related with gender, ancestry and human variation.

1.1.2 Similar Applications and Studies

To the best of the authors' knowledge, no other tool (or set of tools) with the desired functionality exist. That fact adds more importance to the work developed since, besides its applicability, it is a new approach, and that can make the difference in terms of innovation introduced. The possible downside is that not existing any software to compare with, might be somewhat difficult to make a set of tools that can be easily used by *non IT* specialists. That relates, essentially, to their usability. On the other hand, it is positive in the way that with no comparisons to make, there was a greater freedom to develop the tools following the anthropologists needs.

There are some other studies in the forensic science, mainly in the skull reconstruction and feature extraction, in order to obtain information about age, gender, nutritional status or even general level of health. One of those studies was made by Park et al[16]. They used scanners with laser technology to make the acquisition of the skulls with the help of an attached stylus to record the position and orientation. Their goal was to investigate the intra- and inter-examiner reliability when using a laser scan to acquire skulls, i.e. be used in craniometry analysis, and compare the results with the traditionally obtained (manually) by the specialists. It must be noted that, in their work, no landmark points detection was created. The points of interest were all indicated (with a stylus), method similar to manually picking all of the feature points. They have concluded that the method was very useful and with excellent intra- and inter-reliabilities for craniometric studies. This procedure, at least as the literature is concerned, is the choice to make acquisition, with some appended extra information, used to make craniometric studies.

Other studies were made on a topic not directly related (and not derectly aplicable) to cranimetric studies, but still relevant: the model alignment. The alignment, as will be explained later on the document, has an important role on the subject. One method was presented by Chaouch et al [17], based on the analysis of the reflective symmetry and the local translational symmetry along a direction. They have concluded that the proposed method was able to find a rotation that best aligns the 3D models in analysis. This method must be considered as of general use, i.e. for any type of 3D shapes.

Another study, and still considering the alignment of the models, was made by Cheng et al[18]. They focused in the automatic identification of two craniometric planes to, as a further step, automatically align the 3D models. The two planes were the *Frankfurt* and *Saggital*, since both planes are used to define important landmarks on the skull. Procedurally, they have

registered a template skull model with known landmarks (both planes) to a target skull in order to make the mapping. Then, the algorithm iteractively refined the landmark locations according to their medical definition, aiming the best accuracy possible. They concluded that the method was more accurate than symmetry-based methods.

1.2 Document Structure

THIS document is structured in three main sections, besides this chapter.

The first part (chapter 2) is devoted to the description of the craniometry as a science and method, the points and, as well, the measures of interest to make the characterization of the models under study.

Throughout the second part (chapter 3) the complete implementation process is explained. Topics as the technologies through the development process, the chosen architecture for the application, user interface and algorithms of the software are covered.

Finally, there is a third part (chapters 4 and 5) focused on the obtained results, teir discussion and conclusions.

2

Traditional Craniometric Analysis and Tools

THIS chapter is devoted to the analysis of the case study, reference to the tools currently used by the anthropologists, description of some inherent concepts relative to the technologies used on the acquisition process and a brief description of the points and measures of interest.

2.1 Case Study

IN 2009, a iDryas team performed a rescue excavation at Vale da Gafaria (Leprosarium Valley), a site located outside the medieval and modern walls of the Portuguese city of Lagos [19], [20]. This site (15-17th centuries) revealed two occupations. Part of Lagos Leprosarium, only known from historical documents, was excavated. The related necropolis was also identified, with 11 individuals recovered [19], [20]. But, the most significant occupation was an urban discard deposit with an area of more than $1500m^2$ and a stratigraphic thickness superior to 6 meters. Among discarded objects, an important amount of human remains were exhumed (155 individuals, including children).

The skulls collection is composed by 65 cranial and mandibular remains of 60 slaves and 4 leprosy suffers. All of them had an age of death superior to 18 years old. From the 64 remains, 20 are from males, 30 from females and 14 were not determined. Also, worth of mention, is the preservation: 38% have the skulls and mandibles complete, 14% were manually reconstructed (by the anthropologists team) and 48% were fragmented. The fragmentation leaded to the missing of some anatomical portions, and represents an additional challenge (as it will be described later in the text).

Considering the worldwide lack of osteoarchaeological series that could illustrate the earliest phase of the European Atlantic expansion [8], the preliminary research results obtained from the Lagos site are a pioneering attempt to characterize African slaves. The vast majority of the excavated necropolises relevant for the history of the modern Atlantic commerce of African slaves dates from later periods (17th-19th centuries) and was found in the New World [21]. Moreover, only occasionally have the anthropological analyses of African slaves' populations been extensive [8]. Furthermore, only direct observation of the osteological specimens was performed, 3D imaging techniques proposed in this project are unprecedented.

2.2   3D Scanning

THREE dimensional scanning is nowadays an established technology, capable of producing high precision tridimensional digital models for documentation of the reality through *Reversed Engineering*, thus being particularly adapted to cultural heritage remains documentation [22], [23]. *Reversed Engineering* provides powerful, non-destructive R&D tools for the objects' microscopic analysis, allowing a rigorous measurement of their features, surface geometry, texture and volume, using virtual examination, i.e. not requiring repetitive contact with their surface. The preservation of the objects' original physical integrity is especially important in fragile human osteoarchaeological remains. Moreover, this technique also induces the development of new multidisciplinary scientific collaborations, as it allows the swift dissemination of the information, even to geographically distant researchers.

A 3D scanner is a device that analyzes a real-world object or environment to collect data on its shape and possibly its color. The collected data can then be used to construct digital three dimensional models. The purpose of a 3D scanner is usually to create a point cloud of geometric samples on the surface of the subject. These points can then be used to extrapolate the shape of the subject (a process called reconstruction). If color information is collected at each point, then the colors on the surface of the subject can also be registered. 3D scanners share several traits with cameras. Like cameras, they have a cone-like field of view, and like cameras, they can only collect information about surfaces that are not occluded. While a camera collects color information about surfaces within its field of view, a 3D scanner collects distance information about surface within its field of view. The *picture* produced by a 3D scanner describes the distance to a surface at each point in the picture. This allows the three dimensional position of each point, in the picture, to be identified. Figure 2.1 shows a setup of a structured light scanning system.

For most situations, a single scan will not produce a complete model of the subject. Multiple scans from many different directions are usually required to obtain information about all sides of the subject. These scans have to be brought in a common reference system, a process
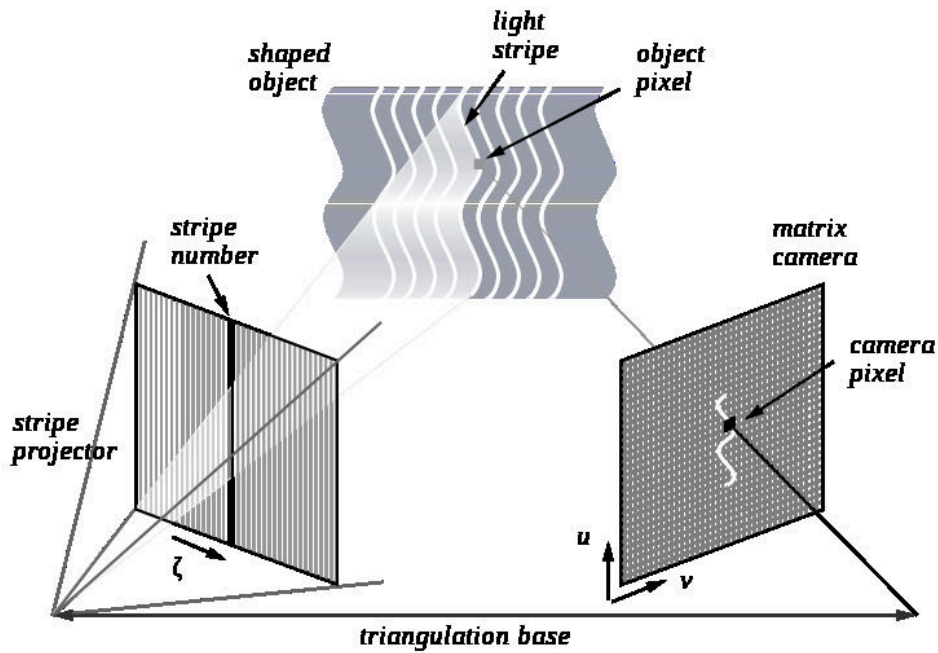
Figure 2.1: Example of structured light scanning system

that is usually called registration, and then merged to create a complete model[24].

There are a variety of technologies for digitally acquiring the shape of a 3D object. A well established classification[25] divides them into two types: contact and non-contact 3D scanners.

Non-contact 3D scanners can be further divided into two main categories, active scanners and passive scanners.

- Contact: probe the subject through physical touch, while the object is in contact with or resting on a precision flat surface plate or on the ground.

- Non-contact:
  - Active: emit some kind of radiation or light and detect its reflection or radiation passing through the object in order to probe an object or environment. Possible types of emissions used include light, ultrasound or x-ray.
  - Passive: do not emit any kind of radiation themselves, but instead rely on detecting reflected ambient radiation. Most scanners of this type detect visible light because it is a readily available ambient radiation. Other types of radiation, such as infrared could also be used. Passive methods can be very cheap, as in most cases they do not need particular hardware but simple digital cameras.

A structured 3D light scanner is a non contact, active device for measuring the three-dimensional shape of an object using projected light patterns and a camera system[26]. Two main methods are mostly used:

7

1. Projecting a narrow band of light onto a three-dimensionally shaped surface. That produces a line of illumination that appears distorted from other perspectives than that of the projector, and can be used for an exact geometric reconstruction of the surface shape (light section).

2. A faster and more versatile method is the projection of patterns consisting of many stripes at once. This allows for the acquisition of a multitude of samples simultaneously. Seen from different viewpoints, the pattern appears geometrically distorted due to the surface shape of the object.

Although many other variants of structured light projection are possible, patterns of parallel stripes are widely used2.1. The picture shows the geometrical deformation of a single stripe projected onto a simple 3D surface. The displacement of the stripes allows for an exact retrieval of the 3D coordinates of any details on the objects' surface.

Two major methods of stripe pattern generation have been established: Laser interference and projection.

1. Laser: the laser interference method works with two wide planar laser beam fronts. Their interference results in regular, equidistant line patterns. Different pattern sizes can be obtained by changing the angle between these beams. The method allows for the exact and easy generation of a very fine pattern with unlimited depth of field. Disadvantages are high cost of implementation, difficulties providing the ideal beam geometry, laser typical effects as noise and the possible self interference with reflection from other objects.

2. Projection: the projection method uses non coherent light and basically work as a video projector. Patterns are generated by a display within the projector, typically an LCD (liquid crystal) or LCOS (liquid crystal on silicon) display.

An essential procedure is the calibration to compensate geometric distortions by optics and perspective. The methods consists in using special calibration patterns and surfaces resorting in mathematical models to describe the imaging properties of projector and cameras.

2.3 Skulls Acquisition

THE acquisition of the 3D skull models on this project was performed using a structured light scanner (Breuckmann Smartscan see Figure 2.2). The acquisition was done by a team from iDryas, including 3D acquisition technician and athropologists, to ensure that important sections of the skulls are acquired and to define a methodology that can be easily repeated in the future. The scanner is sensitive to natural light so the scans were digitized

Figure 2.2: Breuckman 3D Scanner

under controlled light conditions.

A methodology was refined in order to acquire as much detail as possible with as few scans as possible. Most of the scans are made from an inferior view of the skull, specifically the teeth area. As the scanner works in stereo mode there is a limitation on the depth of the acquired surface.

Proprietary (software) application of the sensor was used to register all range images and texture images together to provide a complete 3D model of the skull under study. Figure 2.3 shows a skull resulting from an acquisition. This model was processed from 21 scans with the 3D sensor. The final textured triangular mesh is composed of about 1.5 million triangles with an error below $30\,\mu m$ and is encoded using the PLY (polygon) file format. The PLY format describes an object as a collection of vertices, faces and other elements, along with properties such as color and normal direction that can be attached to these elements. It allows to store some properties related to the object like color, surface normals, texture coordinates and transparency. The expected error depends mainly on lighting conditions and characteristics of the surface being scanned.
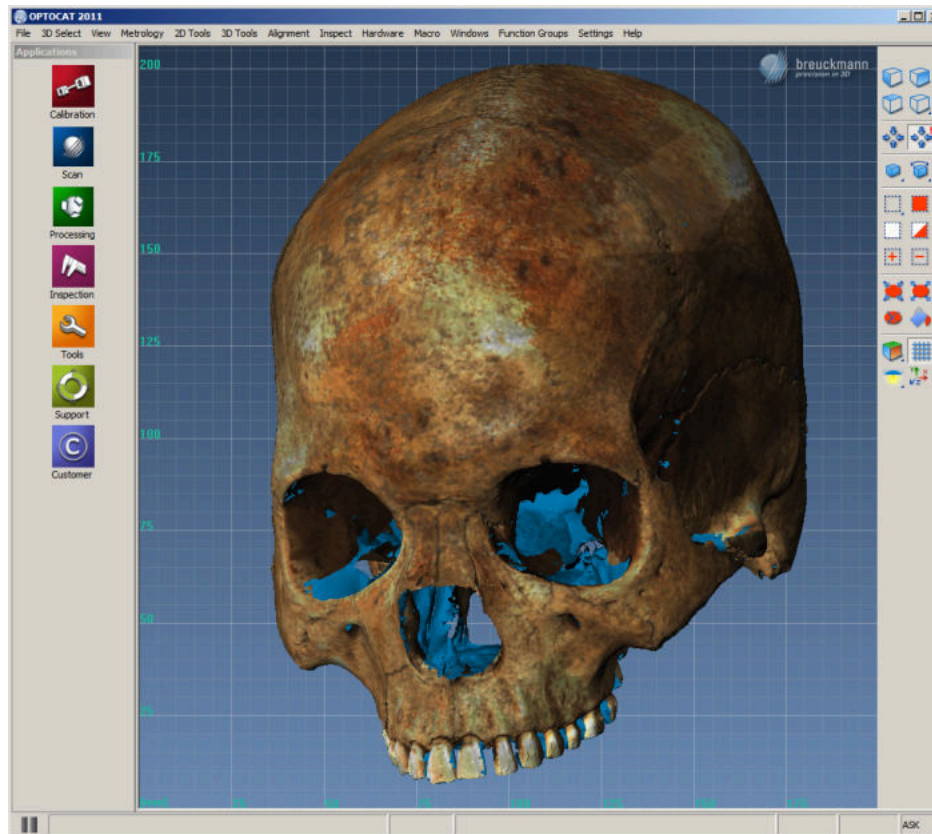
Figure 2.3: Acquired skull from the Breuckman Smartscanner - proprietary software

2.4 Points and Measures of Interest

DEFINING the points of interest to be further used to compute the measures is an essencial requirement. In craniometry many craniometric points are well defined and established as standard use for classification. The anthropologists at iDryas have defined, from the set of points aforementioned, a total of 16 points (see appendix A to get a full list and description) as being of interest for the intended classification. With those 16 points they could get a total of 20 measures (see appendix B for more detail) to be later used to skul classification.

The measuring system, following the traditional methodologies, is always susceptible to the introduction of some error on the measures. Observational error (or measurement error) is the difference between a measured value of quantity and its true value [27]. During the manual analysis of the skulls two typed of errors must be considered:

1. Inter-observer error: the differences between interpretations of two or more individuals making observations of the same phenomenon.

2. Intra-observer error: the differences between interpretations of an individual making observations of the same phenomenon at different times.

As previously mentioned, one of the main expected benefits in developing a method of acquisition and further digital analysis of the skulls is to assure repeatability of the results and, at same time, reducing the measurement error. Also, if possible (what it is firmly believed), reduce the (inter- and intra- observer) variability introduced by the (multiple) manual measurements.

The iDryas team has been using the FORDISC [28] software to classify the skulls. FORDISC is an interactive discriminant functions software created by Stephen Ousley and Richard Jantz [28], widely used by forensic anthropologists to assist in the creation of a decedent's biological profile when only parts of the cranium are available. The program compares potential profiles to data contained in a database of skeletal measurements of modern humans. The functionality falls in the classification of unknown adult skulls on its ancestry, sex and height based on the reference samples which are stored in a database. Discriminant functions are used to construct a classification matrix, and thereby attempts to reach the population group that has more similarities with the unknown individual.

Application - CraMs

3.1 Architecture

T HE developed application, stands for CraMs, is conceptually organized according to figure 3.1. The acquisition process of the skulls follows the procedure explained in Section 2.1. After loading the 3D model, it is necessary to align it. This procedure can be fully manual or semi-automatic. With the aligned model, it is possible to detect some craniometric points of interest. The developed methods allow manual, semi-automatic and fully automatic selection of landmark points. Finally, based on points obtained, the measures
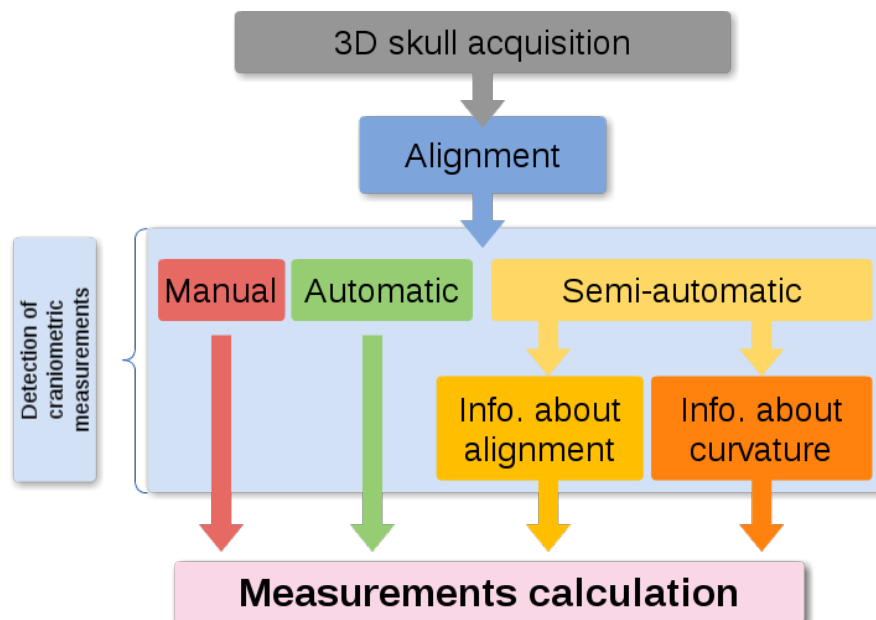
Figure 3.1: Work flow of the application

can be calculated and further analysed by the specialists or, recurring to some classification

software like FORDISC[28].

Figure 3.2 shows a brief but concise view of how the application is structured. Both VTK and Qt are on the top of the Operating System specific code (endianess, file system, etc). Messages are exchanged between both VTK and Qt in order to make possible the APIs' integration (interaction, visualization, windowing system, etc). Concurrently, messages are exchanged between both APIs' and the Operating system (system calls) to make possible the handling of platform specific tasks. The application is on top of both APIs' in use and information is exchanged relatively to the GUI, interaction, visualization, etc. The application layer shows the distinction between four modules:

1. Developed tools: the methods developed to analyse the models, find points of interest, take care of the alignment, etc.

2. GUI: the graphical user interface containing all of the Qt code to handle the window creation, menus, etc.

3. Interaction: contains the code to handle the interaction with the loaded models. Widely used VTKs' functionality.

4. Utils: some utility classes and functions.
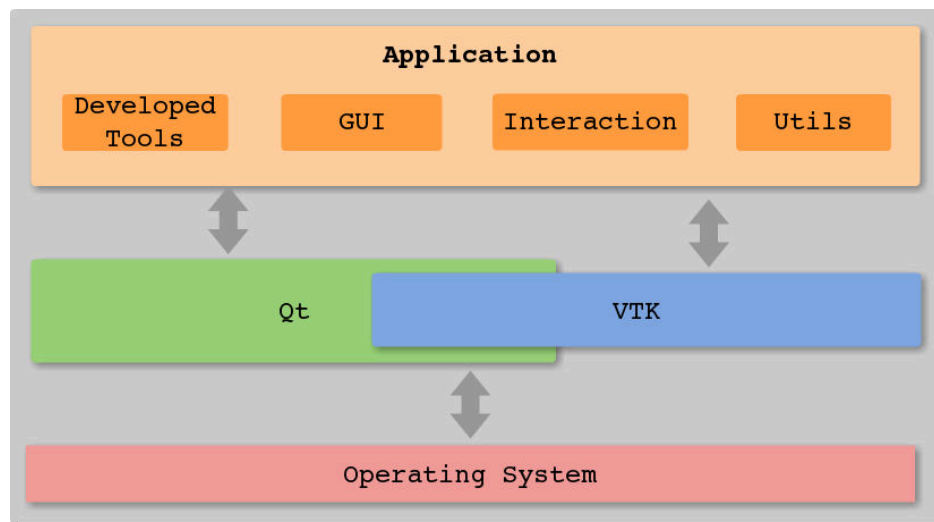
Figure 3.2: Application architecture

14

3.2 Programming Language and APIs'

THE application was developed using the C++ Programing Language. Qt was used for the user interface and VTK for the 3D visualization and interaction. Currently, the application runs on both Microsoft™Windows®and GNU/Linux Operating Systems. Since the building system relies on CMake and the code was written in a way of providing portability it can easily be built in other platforms (e.g. MacOS).

C++ was chosen as programming language as it is a industry standard programming language and makes it possible to create high performance applications. Another reason worth of mention is that all of the possible frameworks that I could use to help in the visualization task (VTK - Visualization Toolkit and PCL - Point Cloud Library) where developed in C++ and, naturally, the main API provided by both relies on it. VTK was the choice to help in the visualization and interaction tasks. It is an easy to use framework and, at the same time, powerful in terms of functionality provided. CMake allow easily build cross platform applications and can be used together with GNU make, Apple XCode and MS Visual Studio. By so, was the chosen building system. Depending on the platform, building tool and compiler, CMake generates the appropriate makefile and/or project configurations. As previously mentioned, Qt was used to develop the user interface. Is a cross platform framework widely used and easily integrated with VTK. The software, as it is, is supposed not be a commercial product and, consequently, no licences were needed to used the Qt framework.

3.3 Alignment

3.3.1 Related Work

THE acquisition process in traditional craniometry does not take in consideration the alignment of the skulls. The anthropologists do not care about the alignment, as they just need to manipulate the skull in a way they can take the measures. To do so, they follow the definition of three planes (based on the three anatomical planes): *Saggital*, *Coronal* and *Frankfurt* (see figure 3.3). These are specifically defined for the craniometry science and have the following characteristics[29]–[31]:

- Saggital: a vertical plane dividing the skull into 2 symmetrical right and left halves, when viewed from the anterior aspect.

- Coronal: divides the skull into anterior and posterior compartments along the Auricular

lines.

- Frankfurt: a plane passing through the inferior margin of the left orbit (the point called the *left orbitale*) and the upper margin of each ear canal or external *auditory meatus*, a point called the *porion.*

These three planes are extensively used in the analysis of the skull[32]. From that, and since it is defined as an essential step in manual craniometric studies, it is a natural conclusion that all of the models must be aligned, e.g, placed in the same 3D referencial before any computerized analysis can be made. Normalization of 3D models (alignment) is a common processing stage (pre-processing, actually) in many applications related to computer graphics such as visualization, recognition and shape matching/retrieving. Taking in account its' importance, a few methods were developed by other authors (explained in further sections). Before focusing on the most relevant methods, it is important to define what is the alignment: a concatenation of isometries (rigid body transform) in 3D space that are used to determine the canonical coordinate system. Usually the center of gravity is chosen and compared to the origin (the origin assures translation invariance). The distinction between two different types of alignment should also be clarified:

1. best alignment between two 3D models;

2. computation of a global coordinate system to all of the models to work with, i.e. have the same coordinate system.

The last, computation of a common coordinate system, is the one of interest in this work.

Before going into more detail about the alignment process it is of great importance to distinguish between three types of alignment:

1. Manual - as the name suggests, the alignment is totally manual. The user must specify a set of points to define the three anatomical planes in order to be possible the computation of the 3D transformation and consequently transform the 3D position of the model to a pre-defined global coordinate system.

2. Semi Automatic - it means that, from the user perspective, she/he is freed of the picking a set of points task. The interaction is reduced to the minimum possible and the advantages are considerable: less work for the user and, as well, better repeatability, accuracy and ease to use.

3. Automatic - fully automatic alignment. The user has no need of intervention in the process. This could be the ideal and, also, a task of most difficulty to accomplish.

3.3.2 Manual Alignment

THIS approach is simple and easy to develop. The user is responsible to provide (pick) a set of landmark points to be used in the alignment axis and, consequently, compute a 3D transformation to be used in the alignment process.

In collaboration with the anthropologists, a set of 7 points were established to be used in the definition of the three alignment axis. The number 7 came as being the minimum number of points needed since a plane can be defined by 3 points or by a point and a normal vector. Two planes were defined with 3 points each and one plane was defined with the remaining point an a vector perpendicular to both previously defined planes. The setting was:

1. Saggital plane - defined with the basion, nasion and bregma points.

2. Frankfurt plane - defined with the orbitale and both left and right porions

3. Coronal plane - defined with the union point and a vector perpendicular to both Saggital and Frankfurt planes (cross product between both).
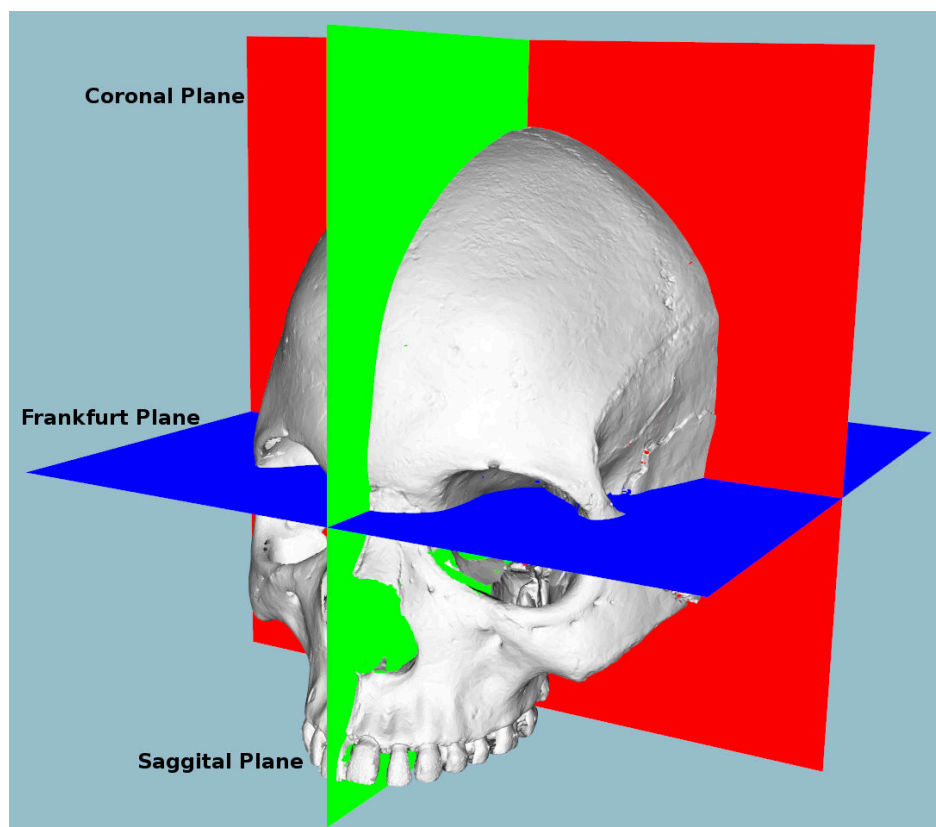
Figure 3.3: The craniometric planes

After defining the three planes, the transformation could be calculated and the model aligned. The alignment, as expected, was correctly made and this approach was maintained as the

solution for manual alignment. The biggest disadvantages of this method are directly correlated to the user: the poor repeatability (since the alignment hugely, depends on the user) and a considerable effort to pick all the 7 points.

3.3.3 Automatic Alignment

BASED on a literature review, it was concluded that the most well-known approach for computing the alignment of 3D objects automatically is based on the *Principal Component Analysis (PCA)* [33]–[37]. The method is a mathematical procedure that uses an orthogonal transformation to convert a set of values belonging to a possible set of correlated variables into a set of uncorrelated variables. These are designated as *principal components* and the number of computed componentes is less or equal to the number of original variables. As the result, the first component has the highest variance and, each of the remaining calculated componentes, in turn, have the highest variance possible under the constraint that they will be ortogonal with the preceding ones. That assures the uncorrelation of the components. Specifically in this case, the method is based on the computation of moments of 3D models[38]. After a translation of the center of mass to the origin of the coordinate system, three principal axes computed with PCA are used to determine the orientation. The experiences presented by the authors just cited show that *PCA alignment* has two disadvantages:

- It is often imprecise and can produce poor alignments;

- The principal axes are not always good at aligning orientations of different models within the same semantic class.

Podolak et al[39] introduced a planar reflective symmetry transform (PRST) that computes a measure of the reflectional symmetry of a 3D shape with respect to all possible planes. They use it to define two new concepts for the global coordinate system: the center of symmetry and the principal symmetry axes. Principal symmetry axes are the normals of the orthogonal set of planes with maximal symmetry, and the center of symmetry is the intersection of those three planes. This approach has been improved by Rustamov with the augmented symmetry transform [40]. Other methods finding symmetries in 3D models have been presented. Minovic et al[41] computed symmetries of a 3D object represented by an octree. Their method is based on the computation of a principal octree aligned with the principal axes. Then they compute a measure of symmetry, the symmetry degree, reasoning with the number of distinct eigenvalues associated to the principal axes. Sun and Sherrah [42] converted the symmetry detection problem to the correlation of the Gaussian image. Then rotational and reflectional symmetry directions are determined using the statistics of the orientation histogram.

An interesting method was developed by Chaouch and Verroust-Blondet. First they make a discrete detection of plane reflection symmetries and classify a model in terms of its symmetry group and the number of its mirror planes. This classification is used to select the good alignment axes among those found by the principal components analysis. Then they introduce local translational invariance cost (LTIC) that measures the invariance of a model with respect to local translation along a given direction. This measure is used to compute the remaining alignment axes when the model has at most one good alignment axis given by the PCA [17].

Another interesting method was developed by Cheng, Leow and Lim[18]. They have focused their work in the alignment of 3D Models of skulls and tried to automatically identify the *Frankfurt* and *Saggital* planes. Their approach consisted in the registration of a template skull model with known landmarks to a target skull to locate the landmarks (the two planes) on the target skull. Then, it iteratively refines the landmark locations according to their medical definition.

PCA

A<small>N</small> experiment was made in order to find out if the PCA could be of good use in the alignment process. The output was a set of 3D axes that were further used to calculate a 3D transformation to align the corresponding model.

Figures 3.4, 3.5 and 3.6 show the Scatter plots for the variables of the original coordinates of the 3D model. Worth of mention is the meaning of the variables A, B and C: A corresponds to the X variable, B to the Y variable and C to the Z variable, in euclidean space. Figure 3.4 shows the comparison between the A and B variables, i.e. the correspondent representation of the XY axis in 3D space. The comparison shown by figures 3.5 and 3.6 depicts the representation of the XZ and YZ planes, respectively.
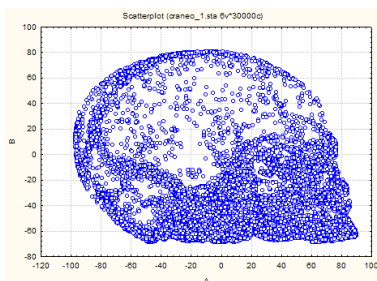
Figure 3.4: Scatterplot for the original coordinates - variables A and B
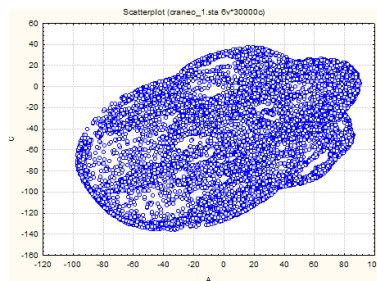
Figure 3.5: Scatterplot for the original coordinates - variables A and C
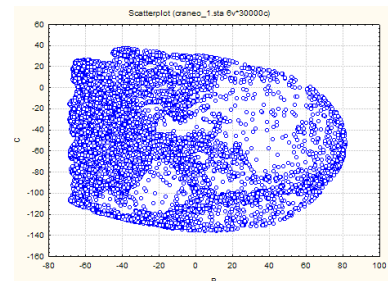
Figure 3.6: Scatterplot for the original coordinates - variables B and C

After the PCA was applied the results depicted by the figures 3.7, 3.8 and 3.9 were obtained. The three factors corresponds to the directions of the three axis expected as output (that will further be used to compute the transformation to apply on the model). Figure 3.8 depicts the eigenvectors of the correlation matrix and 3.9 the values of the factors to use in the aforementioned computation of the transformation.

Value number	Eigenvalue	% Total variance	Cumulative Eigenvalue	Cumulative %
1	1.763450	58.78166	1.763450	58.781656
2	0.725814	24.19380	2.489264	82.975455
3	0.510736	17.02454	3.000000	100.000000

Figure 3.7: Eigenvalues of the correlation matrix (active variables only)

Variable	Factor 1	Factor 2	Factor 3
A	0.619679	0.195494	0.760119
B	-0.523233	0.824769	0.214438
C	0.585001	0.530602	-0.613381

Figure 3.8: Eigenvectors of the correlation matrix (active variables only)

Variable	Factor 1	Factor 2	Factor 3
A	0.822902	0.166551	0.543225
B	-0.694827	0.702660	0.153250
C	0.776852	0.452045	-0.438357

Figure 3.9: Factor coordinates of the variables (based on correlations)

By the analysis of the PCA output it is possible, and useful, to analyse the variables projection on the three different factor-planes. Figures 3.10, 3.11 and 3.12 show that comparison.
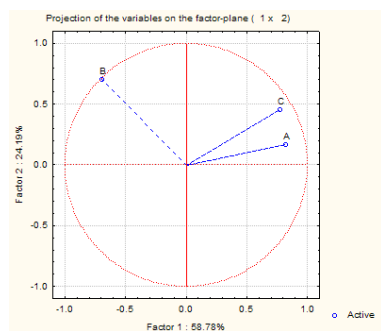
Figure 3.10: Variables projection on the factor plane 1x2
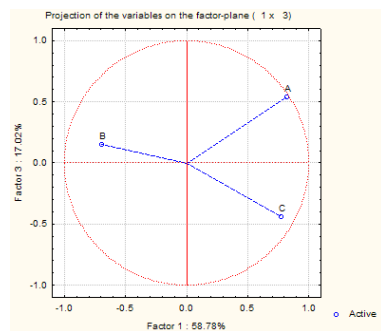
Figure 3.11: Variables projection on the factor plane 1x3
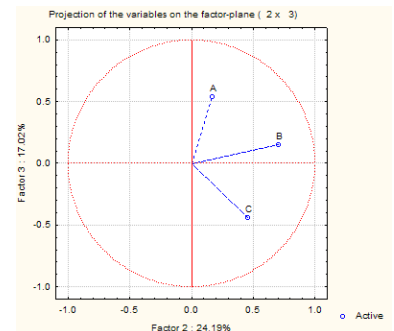
Figure 3.12: Variables projection on the factor plane 2x3

At this point it was not possible to make a statement about the success or failure of the method and the next step implied the computation/application of the 3D transformation. Direct observation has shown that the method, only per si, was not enough to make a good alignment, which confirms other authors previously cited. Due to the complexity of the methods implemented by some authors and no guarantee of good alignment in our case, a semi-automatic approach based on a reference skull was investigated.

3.3.4 Semi-automatic Alignment

THE so called semi-automatic alignment should be considered as an intermediate method to make the alignment of the skull models. The objective was to make a compro-

mise between the advantages and disadvantages of both manual and automatic approaches. Iteractive Closest Points (ICP) [43] was the chosen approach.

ICP - Iteractive Closest Points

I CP is an algorithm developed with the objective of minimizing/registering the diference between two point clouds. The implementation is conceptually simple: interactively revises the transformation needed to minimize the distance between both point clouds.
The algorithm workflow is:

- Associate points according to a nearest neighbor criteria;

- Estimate transformation parameters using a mean square cost function;

- Transform the points using the estimated parameters;

- Iterate until some criteria is met.

VTK, as the version 5.x, provides an implementation of the algorithm and, naturally, was used as a means to make a semi-automatic alignment.

It is now clear that two point clouds are needed as an input to the algorithm. One is the model that should be aligned; The other was defined as being a template model and could be obtained as the result of a manually aligned skull. It can be argued that the manual alignment could introduce some undesired error but, as shown in the results section, the measures obtained with the use of the so-called template model are conformable with the measures obtained with the manual alignment and, on the other hand, with the traditional method used by the anthropologists. The possible way was to start with only a few models (in the worst case only one), make the manual alignment, and save it as a template model to further use in the alignment with ICP. Following that procedure, it could be possible to make a database of template models and use the more appropriate (in terms of geometric characteristics) for the calculation of the transformation. Currently, only a simple version of the idea was implemented: the user may choose the template model but none is stored in a database and, consequently, the best match is used. It may be a step to take into account in future developments.
From the user perspective, the work flow is:

1. The user selects a model to use as template (Figure 3.13);

2. The template model is displayed as a mean of comparison between both skulls (Figure 3.14). An interaction phase is possible; the model to be aligned can be rotated in all 3 axes (angle in steps of ±2.5 degrees) in order to get a good first approximation of the alignment, to compute with the ICP algorithm;

3. ICP is applied and the 3D space transformed skull (only) is shown (Figure 3.15). Observation has shown two possible outcomes:

    a) Accurate and useful alignment;
    b) Completely inaccurate alignment (Figure 3.18). There is no use of the result and the alignment process must be restarted. The user must rotate the model to be aligned in a way that has a relative position (rotation) close to the template model.
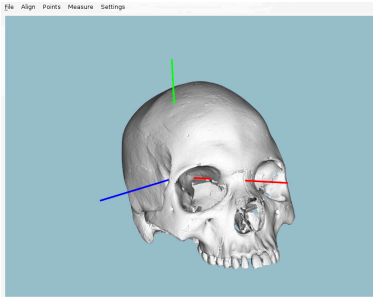
Figure 3.13: Unaligned model
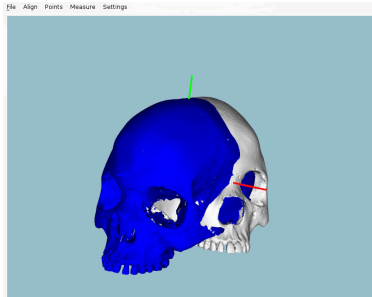
Figure 3.14: Model to align and template model (blue)
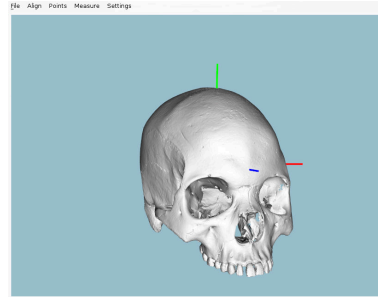
Figure 3.15: Model aligned - ICP was successful

Figures 3.13, 3.14 and 3.15 shows the case of a successful alignment. On the other hand, figure 3.18 shows the opposite case. The computed affine transformation by ICP cannot be used to fulfil the alignment requirements. The case is depicted in the figures 3.16 to 3.18.

Figure 3.16: Unaligned model
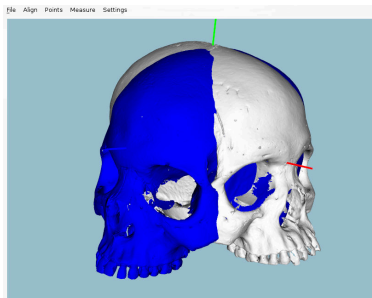
Figure 3.17: Model to align and template model (blue)
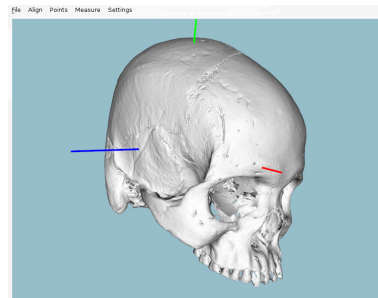
Figure 3.18: Model aligned - ICP algorithm has failed

With the ICP implementation the models could now be aligned in a way that is little influenced by the user interaction and, possibly, guarantees acceptable repeatability.

3.3.5   Discussion

A very considerable amount of effort was made in order to implement/develop the best method to align the models accordingly to the established requirements:

- Correspondence to the defined as three planes by the anthropologists team;

- Robust method, capable of assure repeatability of the results (alignment and consequent landmark points and measures);

- Easy to use.

The manual alignment gets the job done but, as previously mentioned, has some drawbacks if there is the need of using it often. Repeatability problems could easily arise and the accuracy/veracity of the obtained measures compromised.

A fully automatic approach, as mentioned by some authors and concluded from the attempt described earlier in the text, is difficult to implement and there is no guarantee of correct alignments. After some research on the topic, it was decided to follow a semi automatic approach and ICP was the answer. However, the results have shown one of two situations can occur, as the alignment result:

1. Correct alignment;

2. A result far from the desired alignment, i.e. the model is completely unaligned.

It is an important result as the user can easily identify when the algorithm does not produce the desired results and then take the appropriate actions (i.e. refine the position of the model to align by means of rotation of the three axis, X, Y and Z). The fact that ICP works with template models can be also used to make a database of template models and, when the process of choosing the template model, choose the most appropriate from the database instead of requiring the user to choose it. This idea was not implemented in this work but is a strong possibility to be implemented in case of future work.

With the two types of alignment available, the next step was the definition of a set of (initial) points to find. This topic, along with the obtained measures from those defined points, is discussed in detail on the next chapter.

3.4   Methods - Neighbouring and Area Selection

SINCE the first steps on the development that it was clear that having a fully automated system would be too difficult, at least considering the time available to make the dissertation. The main reason is that several feature points correspond to anatomic structures that

might be difficult to detect through an algorithm. However, an interactive system where the experts could provide a region of interest (using a pointing device (*point & click*)) and along a set of rules, defined for each point, could be a good compromise to detect more difficult feature points without the need for precise picking and, at the same time, reducing repeatability problems (the precision would not be dependent of the expert). The same results could be obtained from the (multiple) interaction of different users without compromise the accuracy of the measures. In that perspective, two selection methods were developed:

- Neighbouring: the user can specify a neighbourhood by selecting a point. The system will automatically compute the connected n components of the selected point. For example, with n=5 the application will detect and analyse the neighbours in 5 levels of shared vertices. This technique is illustrated in Figure 3.19 to detect the Nasion. The user selects a point close to the point of interest and the neighbouring region (in green) is automatically searched to find the point closest to the YZ plane, i.e. with the minimum X coordinate value.
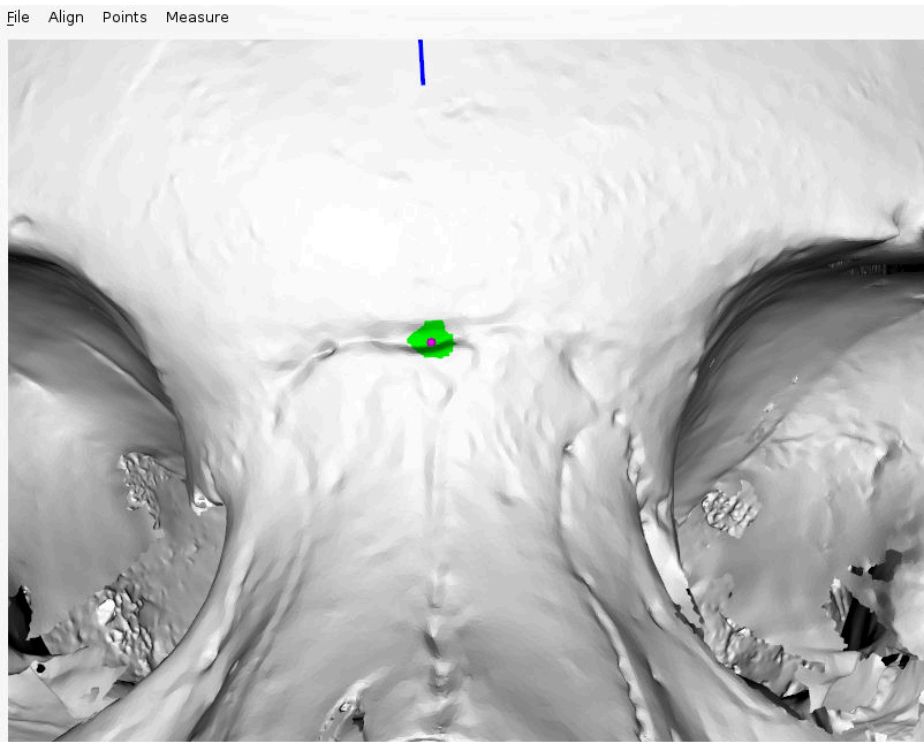
Figure 3.19: Neighbouring algorithm applied to the nasion

- 3D Box Widget: alternatively, users can also provide a region of interest using a 3D Box Widget to indicate volumes of interest. Figure 3.20 illustrates the use of the technique for the detection of the Glabella. The detected feature point is represented in blue. The area selected by the user, making use of the box widget, is represented in

red. The position of the box widget is initialized in a picked position and can then be moved and resized interactively to define the area of search for the feature.

These two methods (neighbouring and box widget) are available to select any feature point given a simple requirement: the point must be the largest or smallest coordinate in one of the 3 axes in the given region. The area of interest can be updated incrementally until the user is satisfied with the resulting detected feature point.
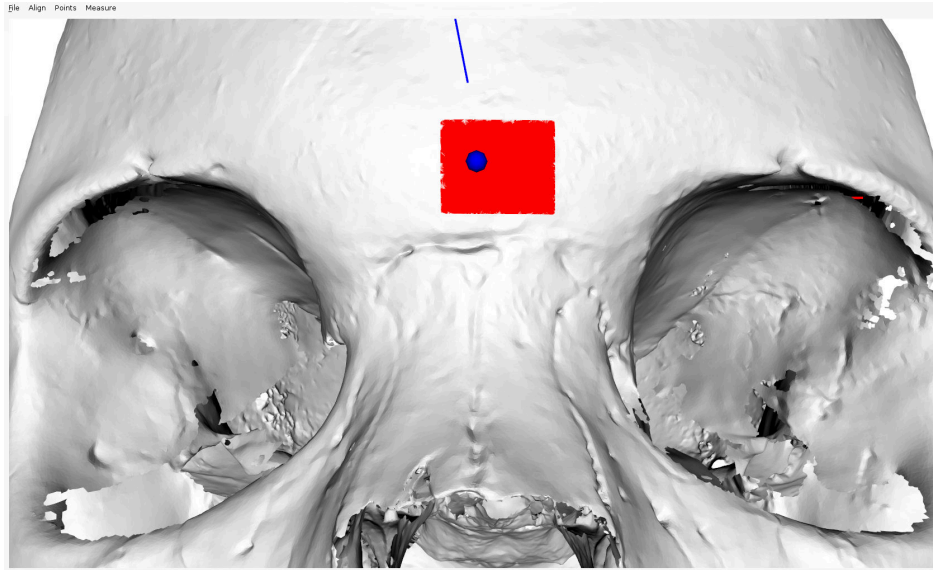
Figure 3.20: Glabella detection using the 3D box widget

Experimentation has shown that the neighbouring method is the most suitable since it provides aproximately the same area of interest as the 3D Box Widget, but is easier to use.

3.4.1 Points

FROM the application of the aforementioned methods, some landmark points were possible to be obtained. The points can be classified as automatic and semi-automatic, correspondingly to the used method.

The following points were found automatically (as depicted by figure 3.21):

1. Zygion (bilateral): Given the aligned skull Zygia are defined as the points with maximum and minimum X coordinates, respectively to the right and left points. Since the zygomatic arch might not be the largest zone of the skull, it is only consider the portion of the skull with negative Y values;
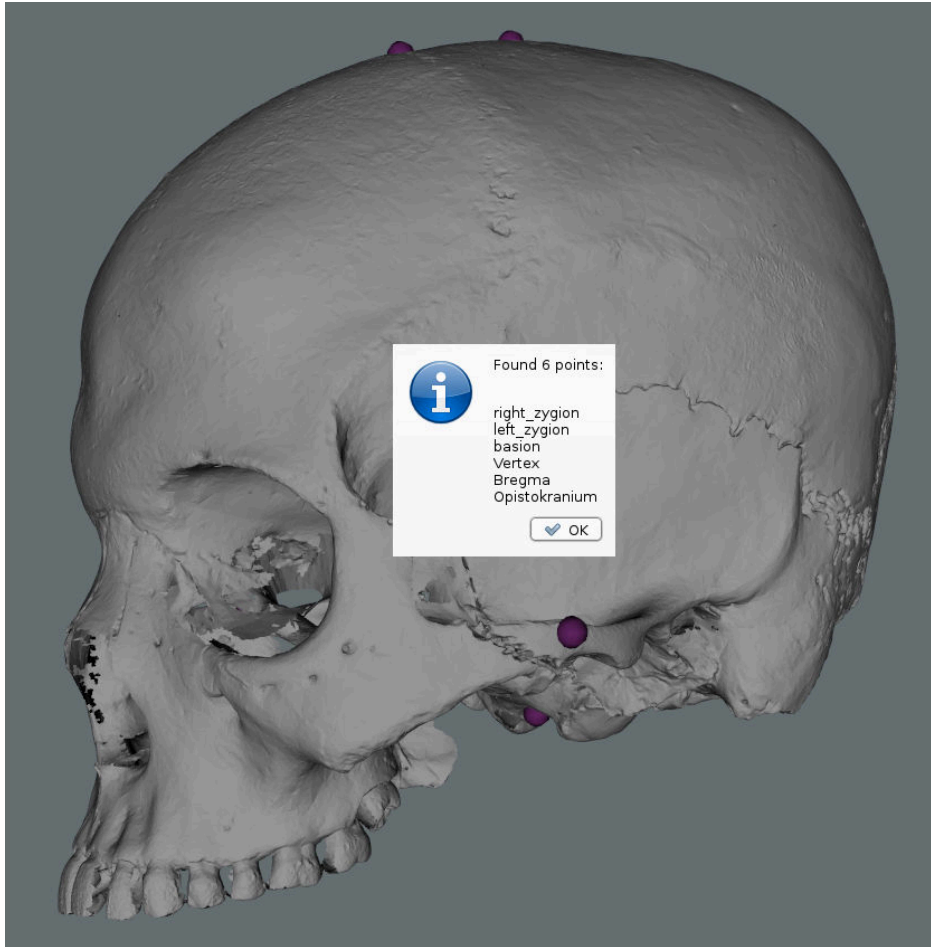
Figure 3.21: Points automatically found

2. Basion: the point is situated on middle border of the anterior margin of the foramen magnum. This feature point is defined as the point with minimum Y coordinate in the Z axis (considering a threshold of ± 0.01 mm in X and ± 0.01 mm in Z coordinates);

3. Vertex: Currently this point is not used to compute any measure, but since it is a point of interest, craniometric wise, and easy to compute we automatically provide it. The point is defined as the highest Y coordinate with the Z and X values within a threshold of ± 0.01 mm;

4. Bregma: The algorithm selects a starting point as the coordinate with greater Y value on the region of points of X and Z within a ± 0.01 mm threshold. Then, it analyses neighbour points in order to find a discontinuity in the Y values, i.e., sudden smaller followed by higher Y values with the aim of finding the coronal suture. Once the suture region is found, the Bregma is selected as point in the region with smaller Y coordinate. Given its simplicity this measure depends heavily on a correct initial alignment since it does not guarantee to find suture crossing. As future work, further improve the algorithm to avoid such dependence from the alignment should be considered.

5. Opisthocranion: The point is simply defined as the minimal Z coordinate value in the Z plane (sagittal), with X varying within a ±0.01 mm threshold.

Both points were found semi-automatically:

1. Nasion: it's determined using one of the neighbouring methods. The search is made for the suture, i.e., the point with smallest Z coordinate value. This point is depicted in figure 3.19;

2. Glabella: the neighboring methods search for the coordinate with highest Z coordinate in the selected region. Figure 3.20 illustrates the case.

3.4.2   Measures

THE measures are defined as being the euclidean distance between two points in 3D space. Based on the, initially found, landmark points (see Points), the system was able to provide directly the following relevant craniometric measurements:

- Facial width (or Bizygomatic Breath)(ZYB): corresponding to the distance between the two Zygia points;

- Height of the skull (BBH): distance between the Basion and the Bregma points;

- Maximum length of the skull (GOL): corresponding to distance between the Glabella and the Opisthocranion;

- Length of the base of the skull (BNL): corresponding to the distance between the Nasion and the Basion;

- Sagittal frontal arc (FRC): Distance between nasion and bregma;

- Maximum cranial breadth (XCB): From the half-back part of the skull, the distance between the two most lateral points.

Tables 3.1, 3.2 and 3.3 show some measures for three skull models (ids number 25, 38 and 65).

		Specialist	Neighbour	3D Box
25	user 1	134	136.7	136.7
	user 2	136	136.7	136.7
38	user 1	120	121.3	121.3
	user 2	119	121.3	121.3
65	user 1	136	136.2	137.2
	user 2	134	136.2	136.2

Table 3.1: Facial Width

		Specialist	Neighbour	3D Box
25	user 1	142	142.6	142.6
	user 2	142	142.6	142.6
38	user 1	133	136.8	136.8
	user 2	122	136.8	136.8
65	user 1	140	137.8.2	137.8
	user 2	139	137.8	137.8

Table 3.2: Height of the skull

		Specialist	Neighbour	3D Box
25	user 1	106	105.4	105.4
	user 2	106	105.4	105.4
38	user 1	95	96.4	96.4
	user 2	95	96.4	96.4
65	user 1	105	105.3	105.6
	user 2	106	105.6	105.6

Table 3.3: Length of the base of the skull

3.5 Curvature and Normal Analysis

3.5.1 Introduction

WITH the objective of getting better results, it was decided that methods as Normal analysis and Curvature analysis of the surface of the models could be of great help. As described by [44], the analysis of the curvature can be used in holistic 3D face detection. Salient face features (i.e. regions) such as the eyes and nose were successfully detected on the 3D models used (150 3D faces acquired by an laser range scanner).

The idea, and taking in consideration the results obtained by [44] was that, since some regions of interest have an accentuated variation in the surface (e.g. the orbital region), a method could be developed with the aim of facilitating the search of landmark points and

regions of interest to be further analysed.

A tool developed at IEETA, PolyMeCo[45], was used to assert the possible relevance of the Normal and Curvature methodologies, since it makes use of those methodologies for polygonal mesh analysis and comparison, as described in [45]. On the specific case of Poly-MeCo, curvature analysis was also used in segmentatiotn of models (zones of high curvature values were boundaries of the segmented parts from the polydata). Experimentation by visual inspection and discussion with specialist has shown that Normal and Curvature analysis could be useful to detect discontinuities on the mesh, as expeced, but no other conclusion could be obtained relatively to landmark points detection and/or precision improvement on the, already detected, landmark points. At this point was decided to further analyse both methods, described next.

In the three-dimensional space, the Normal to a surface at a point P is a vector that is perpendicular to the tangent plane to that surface at P. The concept of normality generalizes to orthogonality. This concept is often used in computer graphics to determine the surfaces' orientation toward a light source (for simple light shading) and/or to determine the orientation of each vertex toward a light source (for more complex shading, designated as Phong Shading[46]).
In the presented case study the values were computed for each vertex and the process will be described in detail bellow in the text.

The other previously mentioned method, Curvature analysis, it is a widely known method to extract information about the type and amount of curvature of a surface. Before going more deep with the concepts behind the curvature analysis is important to define *Principal Curvatures*. Principal Curvatures of a surface at a point are the minimum and maximum of the normal curvatures at that point (Normal curvatures are the curvatures of curves on the surface lying in planes including the tangent vector at the given point.) The principal curvatures are used to compute the *Gaussian* and *Mean Curvatures* of the surface.

- Gaussian curvature: is the product of the principal curvatures at that point;

- Mean curvature: is one half the sum of the principal curvatures at that point.

The results from the application of both the curvature types will produce one of the following results:

1. Negative Curvature - the surface is saddle-like (Figure 3.22);

2. Zero Curvature - the surface is flat in, at least, one direction (Figure 3.23);

3. Positive Curvature - the surface is bowl-like (Figure 3.24).

29
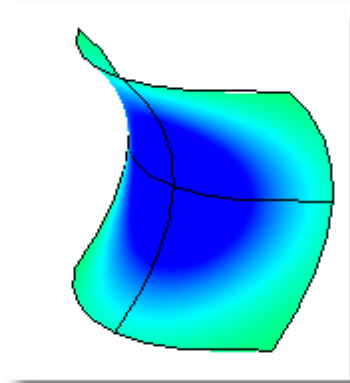
Figure 3.22: Negative Curvature
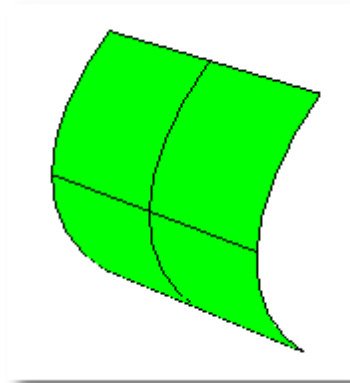
Figure 3.23: Zero (aprox.) Curvature
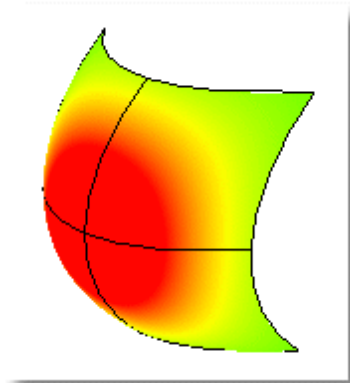
Figure 3.24: Positive Curvature

Illustrations adapted from mcneel.com.

The following two sections will describe the implementation of the Normal and Curvature methods.

3.5.2 Normal Analysis

As previously mentioned, Normal componentes were computed for each vertex of the surface. Given a vertex, a search was made in order to find all connected vertices and, with those, the angles between the vertex and all of the connected were summed. At the end of the iteration the summed value was divided by the number of summed values and the result was stored as being the Normal value for the aforementioned point.

```
getAnglesBetweenNormal(input mesh)
  arrayOfNormalValues : double
    for each point
      neighbourList : array
    sumOfNormal : double
    getNeighbours(mesh) : out = neighbourList
    for each neighbour
      item add angle to sumOfNormal
    sumOfNormal /= numOfNeighbours
    store value in arrayOfNormalsValues
return arrayOfNormalsValues
```

Listing 1: Get angle between Normal vectors for a input mesh
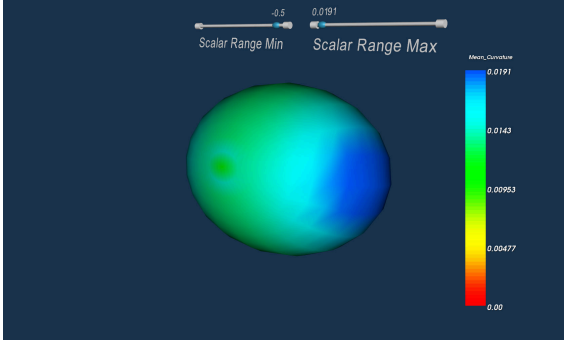
Figure 3.25: Curvature analysis - ellipsoidal mesh
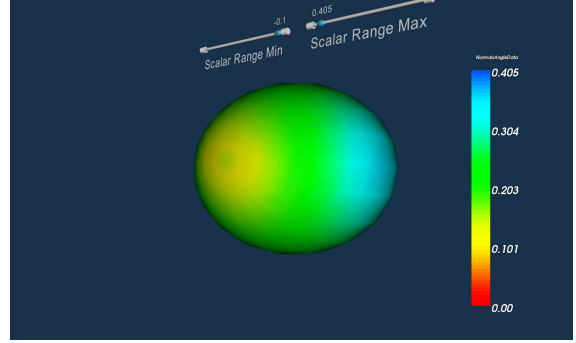
Figure 3.26: Normal analysis - ellipsoidal mesh

With simplicity in mind, the first tests were conducted on a ellipsoid mesh. The aim was to automatically detect points of maximum Normal values that correspond to bowl-like region (i.e. the two extreme regions, resembled to the top and bottom of a egg-like shape). Ir order to distinguish between the possible values of the different regions a color map was applied. The results are depicted on figures 3.25 and 3.26. Values in the order of zero were mapped to the red color. The maximum values were mapped to blue. All of the other values in between. A example of the procedure applied to the skull models is depicted in Figure 3.27.

3.5.3 Curvature Analysis

IN order to find if the analysis of the curvature could provide interesting results, an experiment was done. The implementation used was the one provided by VTK. It allows to choose the analysis of four types of curvature: Minimum, Maximum, Gaussian and Mean. Gaussian and Mean curvatures were previously mentioned. Minimum and Maximum curvatures relates to the corresponding value of the Principal Components, i.e. k_{min} and k_{max}.

$$k_{min} = H - \sqrt{(H^2 - K)} \text{ and } k_{max} = H + \sqrt{(H^2 - K)}$$

The exception of spherical and planar surfaces, which have equal principal curvatures, should be considered. For all directions, the curvature will pass through two extrema: a minimum (k_{min}) and a maximum (k_{max}) which occur at mutually orthogonal directions to

31

each other.

The curvatures algorithm provided as a part of VTK, only *per si*, was not enough to reach any conclusion. Thus, an algorithm was created in a way that, given a input mesh (whole model or a part of it), the type of surface to be taken into account (convex or concave), the coordinates of a starting point (e.g. the picked point), and the number of neighbours to consider, it would return a point that best fit to the requirements. In case of more than one point satisfying the requirements, a centroid point would be returned.
The pseudo code is presented next:

```
getPointMaxCurvature(input mesh)
  compute curvatures for a input mesh
  find initial point, used to start the neighbouring search
  search for n neighbours (connected vertices)
  for each neighbour vertex
    get and store curvature value (map(point, curvature))
  if convex
      compute for convex shape
  else if concave
    compute for concave shape
  if there is more than one point with the same curvature
    compute the centroid of those points
return point
```

Listing 2: Pseudo code for the algorithm to get the point with maximum curvature, taking into account the neighbours

The direct application of the results provided by the curvatures algorithm, in a ellipsoidal model and using a color pallet to represent the values though colors, has shown quite similar results relatively to the Normal analysis. As a further step, the same procedure was applied using the skull models. Results are depicted in Figure 3.28 for the case of the Mean Curvature and in Figure 3.29 for Gaussian Curvature.
Both methods seem to provide similar results. A question arises: could both methods provide the same results for the analysis? Next section will clarify the question and some conclusions will be described.

The analysis of the results obtained using Normal and Curvature analysis, on the ellipsoidal and skull models suggest that both methods could be usefull. With that in mind the decision was to go for the Curvature algorithm instead of the Normal algorithm. The justification is based on the following:

- Curvature analysis is provided as part of VTK and consequent there is a guarantee of good integration with the library and available support;

- Its execution times are in the same order of the *Normal algorithm* (no performance gained).
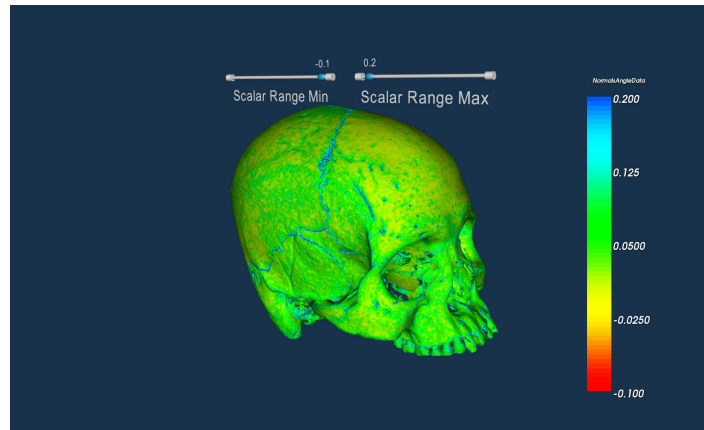
Figure 3.27: Normal analysis
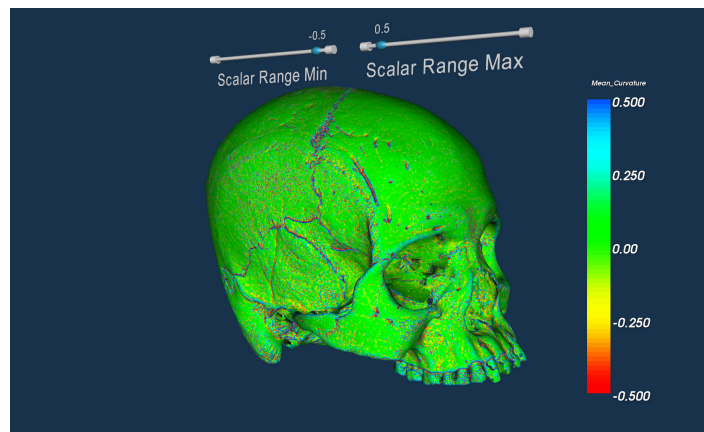
Figure 3.28: Mean curvature

From this point further, the curvatures algorithm started to be used and it should be considered as the default on the text.
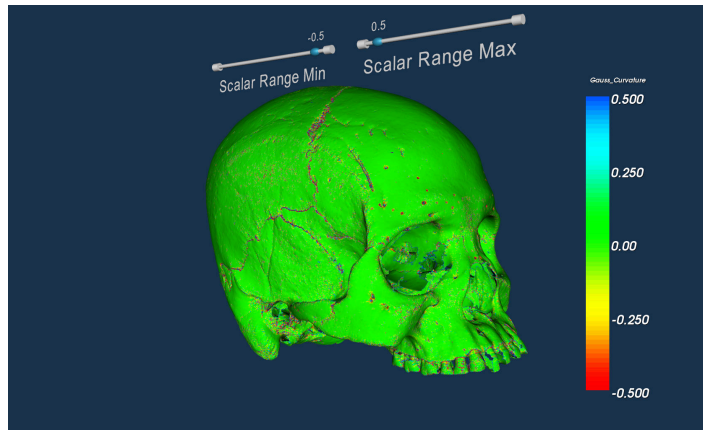
Figure 3.29: Gaussian curvature

3.5.4 Work Flow

Figure 3.30 depicts the flow diagram of the developed application. Detail about the algorithms behind the menu options will be further explained, through the next chapters.
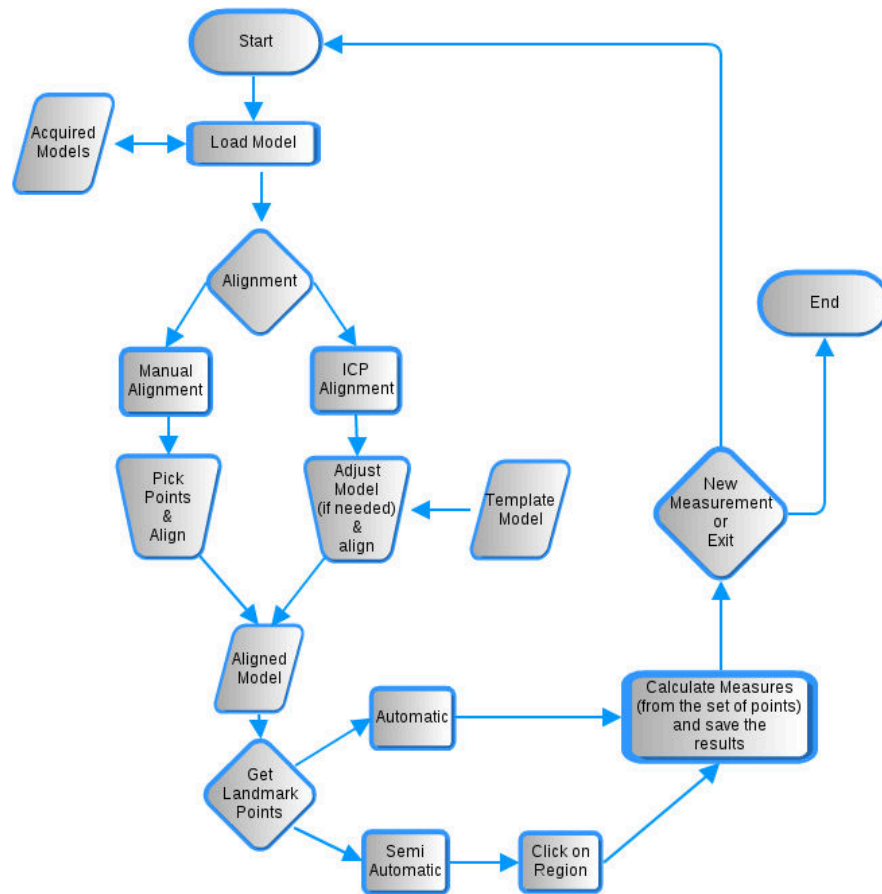
Figure 3.30: Work flow of the application

3.5.5 User Interface

The interface is composed of 5 menus and a few more sub-menus, as it is shown next:

- File: standard functionality in todays' applications, such as opening files and terminate the application;
  - Open File: shows a open file dialog and, when selected a valid model, loads it;
  - Exit: terminates the application.

- Align: functionality related to the models alignment;
  - Manual: if the user selects the manual alignment then she/he must pick the pre-determined set of points used to compute the alignment;
    * Pick Points: allows the user to pick a determined number of landmark points;
    * Align: after the user pick all of the points needed the alignment can be accomplished using this menu.
  - Semi-automatic (ICP): semi-automatic alignment;
    * Load Template: a loading dialog is shown to allow the user being able to select the template model to use on the alignment via the ICP algorithm;
    * Align: the alignment is performed.

- Points: functionality related to the determination of the points of interest;
  - Try Automatic: the application runs a set of algorithms in order to find the most points possible, in a totally automatic procedure;
  - Use Curvature: enables/disables the use of curvature analysis techniques;
  - Glabella: semi-automatic point, the user must choose between one of the provided methods;
    * Neighbouring: the neighbouring algorithm is used;
    * 3D Box Widget: makes use of the 3D Box Widget algorithm.
  - Nasion: semi-automatic point, the user must choose between one of the provided methods. The submenus are the same as the ones available for the Glabella point;
    * Neighbouring: same as before;
    * 3D Box Widget: same as before.
  - Prosthion
    * Neighbouring: same as before.
  - Ectomalares
    * Left;
      · Neighbouring: same as before.
    * Right.
      · Neighbouring: same as before.
  - Biauricular;
    * Left
      · Neighbouring: same as before.
    * Right
      · Neighbouring: same as before.
  - Nasoespinal;
    * Neighbouring: same as before.
  - Frontomallar-Temporalle;
    * Left;
      · Neighbouring: same as before.

* Right.
  · Neighbouring: same as before.

- Measures: calculation of the final measures of interest;

  – Calculate: calculates and displays the measures to the user.

- Settings: Setting related functionality.

  – Preferences: Change the application preferences.

3.5.6 Points

As a result of the Curvature method implemented, the following additional points could now be obtained (depicted in figure 3.31):

1. Prosthion: the landmark point is located between the two superior central incisive teeth and corresponds to the most anterior point in that region. The curvature was applied to find the point with larger curvature in the convex region. Note that the neighbour method can be also applied here but the results would be severely affected by the neighbouring region of search. The curvature method makes possible the discovery of the same point searched in a much bigger region of neighbours and picking area;

2. Left and right Ectomalar: These two points are located over the molars teeth. The region makes bowl-like surface and, once again, a direct application of the curvature method;

3. Left and right Biauricular: Another pair of points that can be considered symmetric (approximately, since the skull is not symmetric). The region corresponds to the start of the *zygomatic process* and has a concave shape. The point of interest is the one with less value of curvature, in both sides;

4. Nasoespinal: Can be found in the bottom of the nasal region. It has a shape of a extreme concave surface and the curvature analysis is able to find it given a large area of neighbouring search (this point has a great repeatability). Once again, since the surface has a concave shape the point corresponds to the smallest curvature value in that region;

5. Left and right Frontomalar-Temporalle: In resemblance to the Biauricular points these two points are amost symmetric (not symmetric because the skull is assymmetric). Can be found in the most posterior and lateral of the frontomalar suture. This region has a shape of a saddle and the curvature algorithm was applied in order to find the point representing the region of largest curvature (convex region).
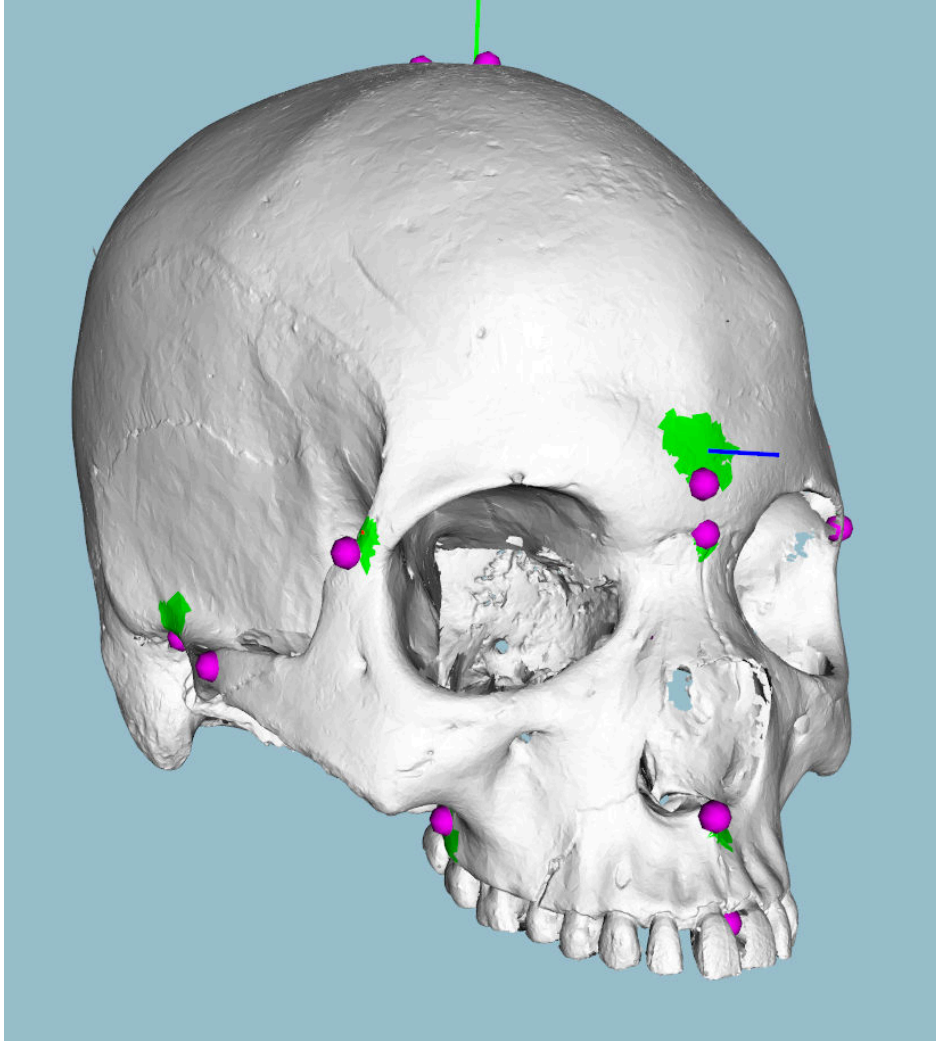
Figure 3.31: Obtained points with the help of all the developed methods (including curvature)

3.5.7 Measures

WITH the points defined, and similarly to the measures obtained relying only on the model alignment, the measure is obtained as the euclidean distance between two points. From the new points found the following measure could be calculated:

1. Length of the skull (BPL): Distance between the Basion and Prosthion.

2. Width of the mandible (MAB): Distance between both left and right Ektomalare points;

3. AUB: Distance between left and right Biauricular points;

4. Superior face height (UFHT): Distance between Prosthion and Nasion;

5. Superior facial width (UFBR): Distance bi Frontomalare-Temporale;

6. Nasal height (NLH): Distance between Nasoespinal and Nasion.

Figure 3.32 depicts all of the obtained measures with this work (total of twelve).
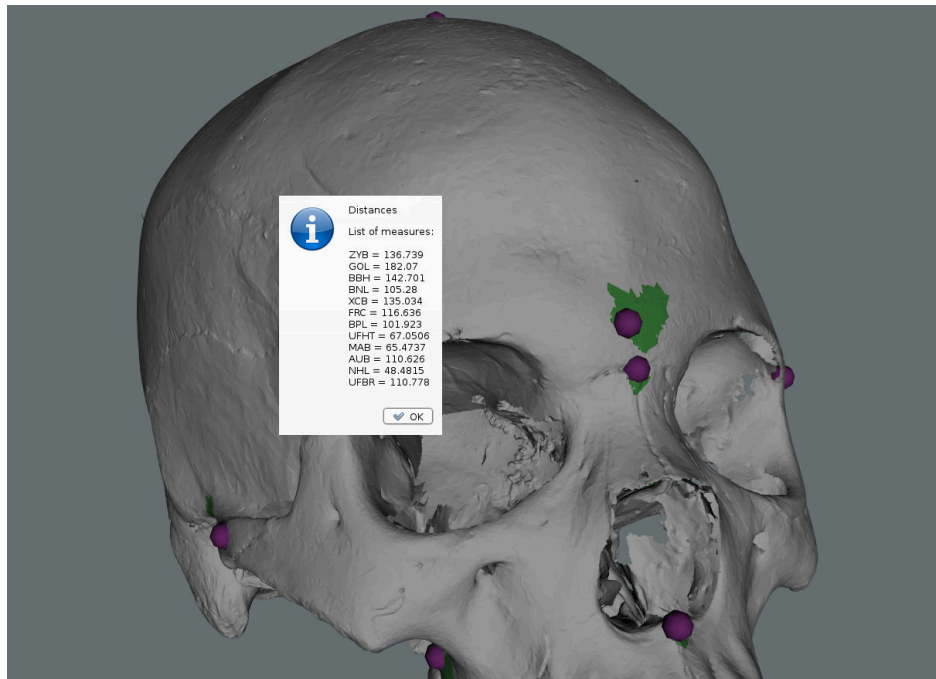
Figure 3.32: Obtained measures

4

Results

4.1 Overview

T HIS chapter aims to present and discuss the results from the developed work. It must be noted that when, except the case of comparing differences between measures, a measurement equals to zero means that was not possible to obtain (probably due to high fragmentation of the skull in study). Firstly, the results about the use of *Manual Alignment* and *ICP* based alignment will be presented. After that, the results about the application of curvature analysis methods with the objective of improving the accuracy and ease to obtain specific landmark points. At the end, the comparison between the measures from the application and the manually ones obtained by the experts (anthropologists), the analysis of the error introduced by both methods and following conclusions.

From the user perspective, the application has the workflow depicted in figure 3.30. After initializing the application the user may load the 3D model to analyse. The next step is the alignment process. It can be manual or relying on the ICP algorithm:

- Manual: a set of landmark points must be picked. As soon as the picking process is completed the model may be aligned;

- ICP: the user may try to make the so-called semi-automatic alignment relying on ICP. The process is as simple as to load a template model and, if needed, adjust the originally loaded model though some rotations (positive and negative angles, in all 3D axis orientations). At the end the model will be in one of the following states: correctly aligned or not. The correct alignment is easily validated and, in the case of incorrect result, the user may restart the process in order to correct it.

With the model correctly aligned, the next step is the calculation of landmark points. Some are totally automatic and the user must use the correspondent application menu to find

them. Next, the other landmark points are obtained in a semi-automatic manner. The user selects an area of interest (i.e. picks a location), where the point is located, and the application searches the neighbouring region for the wanted point. Optionally (and activated by default), the user may use curvature analysis methods in order to try to get more accurate positions for the landmark points.

4.2   Results from the Alignment Approaches

COMPARING only the measures obtained by both methods (table 4.1), the reader may easily conclude that both methods provide results in the same order of magnitude. It may appear that manual alignment might give more guarantees of providing an accurate result. The reason is: if the points are correctly picked the alignment will just work as expected since it is simply mathematically defined (the 3D transformation is well known). On the other hand, the task of picking, over and over, all the seven points used to calculate the aforementioned transformation might be discouraging. Using the ICP method, even though there is always the possibility of failing if the model is too unaligned, the amount of interaction by the user is significantly reduced. Also, in case of failure, the user can easily repeat the ICP based alignment process in order to get the correct alignment. Table 4.1 shows the obtained measures (in millimeters) for two skull models (number 25 and 38). The chosen skull models were number 25 and 38 because, at the time of the initial measurements, those models (from a total of 4 models) were not fragmented. The process was repeated by two different users (user *#1* and user *#2*). The nomenclature *user #* will be used on this chapter to express the distinction between different n users.

	#25				#38			
	user 1	user 1	user 2	user 2	user 1	user 1	user 2	user 2
	ICP	Manual	ICP	Manual	ICP	Manual	ICP	Manual
ZYB	136.7	136.7	136.7	136.7	121.7	121.3	121.7	121.3
GOL	182.1	182.1	182.1	182.1	180.1	180.2	180.1	179.9
BBH	142.7	142.7	142.7	142.9	132.9	138.6	132.9	133.5
BNL	105.3	105.3	105.3	105.3	95.2	98.1	95.2	93.7
XCB	135	135	135	135	137.7	137.7	137.7	137.6
FRC	116.7	116.7	116.7	114.7	109.1	107.5	109.1	108.2

Table 4.1: Comparison of the automatic measures obtained using manual and ICP based alignment. Units are *mm*

4.3 Results from the Curvature Analysis

CURVATURE analysis was employed with the objective of increasing the accuracy and repeatability of the detection of some landmark points. Table 4.2 presents the measures obtained from the neighbouring method applied with and without curvature analysis. It is important to notice that, "Curv1"stands for the measurements obtained for the user designated as being number one making used of the curvature analysis to refine the positions of landmark points and "L.Ext2"stands for the measurements obtained by another user, designated as user two, but using only the extremes in a determined region to compute the positions of the landmark points.

Without comparing to the values manually obtained by domain experts, these results suggest that curvature analysis makes possible the detection of values with meaningly less inter-observer variation.

	#25				#38			
	Curv1	L.Ext1	Curv2	L.Ext2	Curv1	L.Ext1	Curv2	L.Ext2
BPL	102.8	102.5	102.3	101.1	95.9	95.6	95.9	96.6
UFHT	65.6	66.5	66.3	67.8	67.8	67.1	67.8	67.3
MAB*	65.5	66.1	65.4	66.2	61.8	61.8	61.1	61.9
AUB*	111.8	114.7	117.2	115.9	107.6	107.9	108.2	108.3
NLH	48.5	50.2	49.1	49.4	49.9	49.9	52.1	49.4
UFBR	109.5	109.6	109.5	110.3	98.6	98.6	99.3	98.9

Table 4.2: Automatically obtained points from the application of local extremes (minimum or maximum) with and without the help of curvature analysis to refine the obtained points of interest. Units are *mm*

4.4 Craniometric Results and Discussion

TABLE 4.3 shows that, from almost all the obtained measures (twelve), the discrepancy of the results obtained via the developed application and the results obtained by the experts via traditional craniometry can be considered low. The consideration is based on direct observation of the obtained values. As previously stated, it is important to notice that, "App1"stands for the measurements obtained for the user designated as being number one and "App2"stands for the measurements obtained by another used, designated as user two. The same for the iDry label (with the domain expert), respectively. Some exceptions should be noted and will be further discussed.

	#25				#38			
	App1	iDry1	App2	iDry2	App1	iDry1	App2	iDry2
ZYB	136.7	136	136.7	137	121.7	119	121.7	121
GOL	182.1	181	182.1	181	180.1	180	180.1	175
BBH	142.7	142	142.7	143	132.9	133	132.9	133
BNL	105.3	106	105.3	107	95.2	95	95.2	96
XCB	135	131	135	131	137.7	136	137.7	137
FRC	116.7	114	116.7	115	109.1	112	109.1	107
BPL	102.8	103	102.3	104	0	0	0	0
UFHT	65.6	62	66.3	64	0	0	0	0
MAB*	65.5	66	65.4	65	61.8	61	61.1	61
AUB*	111.8	110	117.2	108	107.6	101	108.2	101
NLH	48.5	47	49.1	47	49.9	48	52.1	47
UFBR	109.5	106	109.5	109	98.6	98	99.3	99

Table 4.3: Results - Comparison of the measures obtained from the application and by the experts *mm*

4.5 Inter-observer Evaluation with iDryas Experts

TABLE 4.4 shows the results obtained by the two experts from iDryas, on two skulls, using the difference of measures between both users (inter-observer error) is also shown. Notice the fact that, for skull number 38, two measures (AUB and MAB) could not be accurately calculated as the experts said that since the skull was fragmented the accuracy could be compromised and the results should not be taken into account.

As it can be observed by the results, the inter-observer error is very small. Once again, the fact that the inter-observer error was reduced and the repeatability of the results assured.

In order to quantify the error made through the use of the developed methods, a table repesenting variations of inter-observer measurements was created. The idea was to compare the measures obtained by different users with the ones provided by the experts. The comparison consists in making the calculation of the variation of the measurements, for all skull models under study. Why only the inter-observer case was considered is a pertinent question at this point and the answer lies on the fact the, as being a semi-automatic computerized tool, the intra observer error should be low and might be discarded. The validation was not made for all the models under study but, the small variation between two users and the results observed during the development process (where the same user repeated the process

	#25			#38		
	user 1	user 2	diff	user 1	user 2	diff
ZYB	136.7	136.7	0	121.7	121.7	0
GOL	182.1	182.1	0	180.1	180.1	0
BBH	142.7	142.7	0	132.9	132.9	0
BNL	105.3	105.3	0	95.2	95.2	0
XCB	135	135	0	137.7	137.7	0
FRC	116.6	116.6	0	109.1	109.1	0
BPL	102.8	102.8	0	95.9	95.9	0
UFHT	64.9	65.6	0.7	67.8	67.8	0
MAB*	67.6	67.3	0.3	61.8	61.9	0.1
AUB*	117.2	117.8	0.6	105.4	111.5	6.1
NLH	48.5	48.5	0	49.8	49.9	0.1
UFBR	108.9	109.1	0.2	97.6	97.7	0.1

Table 4.4: Results from two domain experts using the developed application. Units are *mm*

over and over), suggests that the intra-observer error was substantially reduced.

As shown by table 4.4, four cases should be analysed and discussed due to the magnitude of the values. Starting by the values obtained from the application, two cases should be considered:

1. Error in the AUB measure: the variation of the measures is 5.4mm, a value notable on the negative side. The experts from iDryas have obtained a inter-observer error of 2.0mm and, by that fact, the measure should not be considered for the skull in question (number 25). On the skull number 38 the situation was not observed because the error from the semi-automatic method has a magnitude of 0.6mm (higher than the variation observed by the experts, i.e. 0.0mm);

2. The same situation happened on skull number 38 but, this time, for the NLH measure. The application resulted in a variation of 2.2mm between measure while the experts only registered a variation of 1.0mm. After discussing the situation with the experts a conclusion arose: the points used to make the calculation of the measure were incorrectly defined (by the developer).

3. On the positive side, on skull number 25, the measure UFBR has registered a much better result between observers with the use of the application (variation of 0.2mm rather than with the measurements made by the iDryas team (variation of 3.0mm));

4. reference for the measure XCB on the skull number 38. As the previous case, the measurements taken by the application have shown a much lower variation (0.0mm versus 5.0mm).

Table 4.5 shows the variation of the measurements for two skulls (numbers 25 and 38) between the two users (inter-observer) using the application and traditional methods. Note

that both users have made the measurements on the application and recurring to traditional methods and the difference is the absolute value between both measurements (on each case).

	skull #25		skull #38	
	App	iDryas	App	iDryas
ZYB	0	1	0	2
GOL	0	0	0	5
BBH	0	1	0	0
BNL	0	1	0	1
XCB	0	0	0	1
FRC	0	1	0	5
BPL	0.5	1	0	0
UFHT	0.7	2	0	0
MAB*	0.1	1	0.7	0
AUB*	5.4	2	0.6	0
NLH	0.6	0	2.2	1
UFBR	0	3	0.7	1

Table 4.5: The variation (inter-observer) of the measures using the application (App) and traditional methods by the experts (iDryas). The variation was calculated taking in account two measurements of different uses, for each case. Attempts to provide a simple comparison of inter-observer error indicator. Units are *mm*

The analysis shows that, for all of the other obtained measures, the variation was always smaller when using the developed application.

As shown by [47], the most common way to express the error margin in anthropometry is using the *technical error of measurements (TEM)*. The value is an accuracy index and represents the measurement quality. By using it, anthropologists are able to attest the intra-evaluator and inter-evaluator erros. The Anthropologists team (iDryas) adopted this index as a mean to calculate the errors on the measurements and, because of that, it was also adopted to evaluate, and further compare, the results obtained with the application.
The TEM index, which is the standard deviation between repeated measures, allows the estimation of confidence intervals around the actual value of the obtained measurements that include non controllable possible variations. Thus, enables to assess the alterations detected in repeated measurements, either by the same person in different points in time or by two different people.

The calculation can be obtained applying equation (4.1), followed by equation (4.2):

$$Absolute\,TEM = \sqrt{\frac{\sum d_i^2}{2n}} \tag{4.1}$$

$$Relative\,TEM = \frac{Absolute\,TEM}{VAV} * 100 \tag{4.2}$$

where $\sum d_i^2 = $ summation of deviations raised to the second power

$n = $ number of measurements

$i = $ number of deviations

$TEM = $ Technical error of measurement expressed in %

$VAV = $ Variable average value (average of the average between all the observations, for each measure).

The results of the calculation of the relative TEM in the case of inter-observer measurements are shown on table 4.6. The second column, Application, represents the error of the measurements obtained making use of the CraMs application and the third column, Anthropologists, represents the error of the measures obtained with the traditional methods.

Skull #	Application (%)	Anthropologists (%)
21	0.65 %	6.81 %
25	0.33 %	2.62 %
38	7.61 %	12.01 %
39	0.20 %	19.11 %
57	6.88 %	3.96 %
65	2.20 %	7.71 %
66	0.09 %	36.40 %
67	0.10 %	33.52 %

Table 4.6: Relative TEM (mm)

The values represent the relative error for each skull. The application provided measurements with much less error percentage.

All measurements, obtained from 8 skulls, are presented in Appendix C.

5

Conclusion and Future Work

5.1   Conclusion

THE work presented is this dissertation was just a šcratch on the surface, taking into account the complexity of the problem. As previously mentioned, no similar tool exists currently capable of the wanted analysis on the 3D skull models and thus, although the techniques used (normal and curvature analysis, ICP,...) were not novel , their application to this problem resulted in an innovative tool.

The time available to make this dissertation was not enough to develop methods to detect all the points of interest (neither automatically nor semi-automatically). Currently six points are automatically detected (Left and Right Zygion, Basion , Bregma, Vertex and Opistokranium), and ten are semi-automatically detected using neighbouring and curvature methods (Glabella, Nasion, Prosthion, left and right Ectomalars, left and right Biauriculars, Naoespinal, and left and right Frontomalar-Temporalls). With these points a total of twelve measures can be calculated (from a total of 24 iDryas experts would like to have).

The number of obtained measures, twelve, is important not only as it shows the applicability of the developed methods but also, and even more important (one of the main goals and challenges), as it suggests that an adequate repeatability of the measures is attainable. From the set of twelve measures, ten were considered accurate enough and consequently compared to the measures obtained by the anthropologists using traditional methods. The inter-observer variability found for all these measures obtained using the application was substantially smaller than while using traditional methods, leading to the conclusion that the repeatability goal was attained for all the measures that were validated, i.e. considered accurate enough by the domain experts .

In order to demonstrate the applicability of the developed tool, a test was conducted with two domain experts from iDryas. The whole procedure (alignment of the skull models, selection of the semi-automatic points and measure calculation) was performed on two different skull models and the feedback provide by the anthropologists was that the application was able to provide useful and accurate results

5.2 Future Work

A FTER the analysis of the obtained results and testing with some members of the anthropologists team, it is clear that some work remains to be done:

- Utilize the curvature (that it is believed can be useful on the task) to detect regions like the orbits. From that extracted information other measurements could be obtained and, as well, other features useful for the classification of the skulls that are currently not available.

- Develop a method to detect the sutures and, from those, extract its shape and make a proper characterization (according to the guidance of the anthropologists). Useful information can be extracted from the suture analysis, e.g. from the complexity of the line formed by the suture and intersection of different sutures (possibly a point of interest). Once again, curvature analysis could be used as a method to detect the sutures and after that another methodology could be used to extract the desired information. Methods may include shape analysis, intersection and simplification of the suture lines.

- Develop methods to find the remaining points of interest (and by that, calculation of all measures used for the classification). Probably, with the development of the two previously mentioned features, all or almost all of the remaining points can be obtained and, consequently, the measures calculated.

- Improve the alignment through ICP making a database of template modes that would be chosen automatically according to best fitting (in terms of anatomical characteristics) the model to align. It is believed that, as a consequence, ICP would result in better results and reduce the need of user interaction in some cases (trough rotations on the original models).

- Make an atlas of models with the already found points information stored. With the same line of ideology as the previous point, the database of models could be used to, firstly, find the model that best fits the skull in analysis and, secondly, map the points correctly found on the stored model to the model to be analysed and further

used methods like neighbouring to find the correct anatomical positions. This way, the user could be freed of the task of picking some points and, would only need to make the validation of each point. If any of the automatically found points was not correct the user could use the picking procedure to correctly indicate the point. After the processing, the skull model could be stored as a template model to be further used in the atlas database.

- Although the current solution for the alignment works well, the development of a totally automatic method could be addressed, as well, in future work.

- Since some models are fragmented, a method to reconstruct (accurately) the mesh would be of great use.

- The application handle some CPU intensive tasks; Optimization could also be addressed as further work.

Bibliography

[1] W. Howells W., "Cranial variation in man. a study by multivariate analysis of patterns of difference among recent human populations", *Papers of the Peabody Museum of Archaeology and Ethnology*, no. 67, pp. 1–259,

[2] C. C. Stephens, "Measure of truth? an examination of the history, methodology, theory and practice of craniometric analysis: with special focus on its application in forensic identification.", eng, *Totem: The University of Western Ontario Journal of Anthropology*, no. 8, pp. 83–108, 2000.

[3] P. H. Moore-Jansen, R. L. Jantz, and S. D. Ousley, *Data Collection Procedures for Forensic Skeletal Material.* K. D. o.A. University of Tennessee, and K. F. A. C. University of Tennessee, 1994.

[4] H. W.W., "Cranial variation in man; a study by multivariate analysis of patterns of difference among recent human populations.", *Papers of the Peabody Museum of Archaeology and Ethnology Harvard University. Cambridge, Massachusetts.*, vol. 67, 1973.

[5] U. Vioarsdottir, P. O'Higgins, and C. Stringer, "A geometric morphometric study of regional differences in the ontogeny of the modern human facial skeleton.", *J. Anat.201*, pp. 211–229, 2002.

[6] T. Buck and U. Vidarsdottir, "A proposed method for the identification of race in sub-adult skeletons: a geometric morphometric analysis of mandibular morphology.", *Journal of Forensic Science 49(6)*, pp. 1–5, 2004.

[7] S. Sholts, K. Miller, and S. Warmlander, "The application of three-dimensional midfacial profiling in the identification of human skeletal remains.", *Poster presented at the 18th International Symposium on Human Identification. Los Angeles, California.*, 2007.

[8] H. J.T., "Cranial nonmetric variation and estimating ancestry.", *Journal of Forensic Science 54(5)*, pp. 985–995, 2009.

[9] A. Ross, D. Slice, and S. Williams, "Geometric morphometric tools for the classification of human skulls.", *Report to the U.S. Department of Justice.*, 2010.

[10] P. Gonzalez, V. Bernal, and S. Perez, "Analysis of sexual dimorphism of craniofacial traits using geometric morphometric techniques.", *International Journal of Osteoarchaeology 21(1)*, pp. 82–91, 2011.

[11] B. Williams and T. Rogers, "Evaluating the accuracy and precision of cranial morphological traits for sex determination.", pp. 729–735, 2006.

[12] S. Sholts, P. Walker, S. Kuzminsky, K. Miller, and S. Warmlander, "Identification of group affinity from crosssectional contours of the human midfacial skeleton using digital morphometrics and 3d laser scanning technology.", *Journal of Forensic Science 56(2)*, pp. 333–338, 2011.

[13] E. Giles and O. Elliot, "Sex determination by discriminant functions analysis of crania.", *American Journal of Physical Anthropology 21*, pp. 53–68, 1963.

[14] E. Cunha and G. Van Vark, "The construction of sex discriminant functions from a large collection of skulls of known sex.", *International Journal of Anthropology 6 (1)*, pp. 53–66, 1991.

[15] C. Cattaneo, "Forensic anthropology: developments of a classical discipline in the new millennium.", *Forensic Sciences International 165*, pp. 185–193, 2007.

[16] H.-K. Park, J.-W. Chung, and H.-S. Kho, "Use of hand-held laser scanning in the assessment of craniometry.", *Forensic science international*, vol. 160, no. 2-3, pp. 200–6, Jul. 2006, ISSN: 0379-0738.

[17] M. Chaouch and A. Verroust-Blondet, "Alignment of 3D models", *Graphical Models*, vol. 71, no. 2, pp. 63–76, 2009.

[18] Y. Cheng, W. Leow, and T. Lim, "Automatic identification of Frankfurt plane and mid-sagittal plane of skull", *Applications of Computer Vision*, 2012.

[19] M. Neves, M. Almeida, and M. Ferreira, "Separados da vida e na morte: retrato do tratamento mortuário dado aos escravos africanos na cidade moderna de lagos. 7º encontro de arqueologia do algarve.", *XELB 10*, pp. 547–560, 2010.

[20] M. Neves, M. Almeida, and M. Ferreira, "História de um arrabalde durante os séculos xv e xvi: o "poço dos negros" em lagos (algarve, portugal) e o seu contributo para e estudo dos escravos africanos em portugal.", *Câmara Municipal de Lagos*, pp. 29–46, 2011.

[21] "Bioarchaeology of the african diaspora in the americas: its origins and scope.", *Annu. Rev. Anthropol.*, vol. 30, pp. 387–422, 2001.

[22] A. Balzeau, I. Crevecoeur, H. Rougier, A. Froment, E. Glissen, D Grimaud-Hervé, P. Mennecier, and P. Semal, "Applications of imaging methodologies to paleoanthropology: beneficial results relating to the preservation, management and development of collections.", *Comptes rendus Palevol (9)*, pp. 265–275, 2010.

[23] M. Wachowiak and B. Karas, "3d scanning and replication for museum and cultural heritage applications.", *JAIC 48*, pp. 141–158, 2009.

[24] F. Bernardini and H. Rushmeier, "The 3d model acquisition pipeline", *Comput. Graph. Forum 21 (2)*, pp. 149–172, 2002.

[25] B. Curless, "From range scans to 3d models", *ACM SIGGRAPH Computer Graphics 33 (4)*, pp. 38–41, 2000.

[26] B. Furht, "Encyclopedia of multimedia (2nd ed.)", *Springler*, p. 222,

[27] Y. Dodge, *The Oxford Dictionary of Statistical Terms*. OUP - Oxford University Press, 2003.

[28] S. Ousley and R. Jantz, "Fordisc 3.0: personal computer forensic discriminant functions.", *University of Tennessee*, 2005.

[29] J. S. Staubesand, "Atlas of human anatomy", *Baltimore-Munich: Urban & Schwarzenberg*, vol. 1, 1990.

[30] J. Rohen and C. Yokochi, "Color atlas of anatomy", *New York: Igaku-Shoin*, 1998.

[31] K. Moore and A. Dalley, "Clinically oriented anatomy", *Philadelphia: Lippincott Williams & Wilkins*, 2006.

[32] C. B. Pereira and M. C. De Mello E Alvim, *Manual Para Estudos Craniométricos E Cranioscópicos*. Univ. Federal de Santa Maria, 1979.

[33] E. Paquet, M. Rioux, A. Murching, T. Naveen, and A. Tabatabai, "Description of shape information for 2-d and 3-d objects", *Signal Processing : Image Communication*, vol. 16, pp. 103–122, 2000.

[34] D. Vranic, D. Saupe, and J. Richter, "Tools for 3d-object retrieval: karhunen-loeve transform and spherical harmonics", *Workshop Multimedia Signal Processing, Cannes, France*, 2001.

[35] P. Shilane, P. Min, M. Kazhdan, and T. Funkhouser, "The princeton shape benchmark", *SMI'04*, pp. 167–178, 2004.

[36] T. Zaharia and F. Preteux, "3d versus 2d/3d shape descriptors: acomparative study", *SPIE Conf. on Image Processing: Algorithms and Systems, CA, USA*, 2004.

[37] B. Bustos, D. A. Keim, T. Schreck, and D. Vranic, "An experimental comparison of feature-based 3d retrieval methods", *3DPVT'04*, 2004.

[38] E. Paquet, A. Murching, T. Naveen, A. Tabatabai, and R. M., "Description of shape information for 2-d and 3-d objects", *Signal Processing: Image Communication*, vol. 16, pp. 103–122, 2000.

[39] J. Podolak, P. Shilane, A. Golovinskiy, S. Rusinkiewicz, and T. Funkhouser, "A planar-reflective symmetry transform for 3d shapes", *ACM Trans. on Graphics, 25(3)*, pp. 549–559, 2006.

[40] R. Rustamov, "Augmented symmetry transforms", *SMI'07*, pp. 13–20, 2007.

[41] P. Minovic, S. Ishikawa, and K. Kato, "Symmetry identification of a 3-d object represented by octree", *IEEE Trans. Pattern Anal. Mach. Intell. 15(5)*, pp. 507–514, 1993.

[42] C. Sun and J. Sherrah, "3d symmetry detection using the extended gaussian image", *IEEE Trans. Pattern Anal. Mach. Intell. 19(2)*, pp. 164–168, 1997.

[43] P. J. Besl and N. D. McKay, "A method for registration od 3-d shapes", *IEEE Transactions on Pattern Analysis and Machine Inteligence*, vol. 14, no. 2, pp. 239–256, 1992.

[44] A. Colombo, C. Cusano, and R. Schettini, "3D face detection using curvature analysis", *Pattern Recognition*, vol. 39, no. 3, pp. 444–455, 2006.

[45] S. Silva, J. Madeira, and B. S. Santos, "PolyMeCo—An integrated environment for polygonal mesh analysis and comparison", *Computers & Graphics*, vol. 33, no. 2, pp. 181–191, 2009.

[46] D. Hearn and M. P. Baker, *Computer graphics*. Upper Saddle River, NJ, USA: Prentice-Hall, Inc., 1986, ISBN: 0-13-165382-2.

[47] T. A. Perini, G. L. Oliveira, J. d. S. Ornellas, and F. P. Oliveira, "Technical error of measurement in anthropometry", *Rev Bras Med Esporte*, vol. 11, no. 1, pp. 86–90, 2005.

[48] B. C. Pereira and M. C. Mello e Alvim, *Manual para Estudos Craniométricos e Cranioscópicos*.

[49] C. R. S. Coelho, "Uma identidade perdida no mar e reencontrada nos ossos: Avaliação das afinidades populacionais de uma amostra de escravos dos séculos XV-XVI", *Faculdade de Ciências e Tecnologia - Universidade de Coimbra*, 2012.

Appendix A Points

THE following points were defined as the feature points to use in the classification of the skulls:

1. Alveolon (alv): intersection point of the mid line of the palate with the perpendicular tangent to the posterior border of the alveolar arch.

2. Basion (ba): the point is situated on middle border of the anterior margin of the foramen magnum. This feature point is defined as the point with minimum Y coordinate in the Z axis (considering a threshold of ± 0.01 mm in X and ± 10 mm in Z coordinates);

3. Bregma (b): intersection point between the sagittal suture and the coronal suture. The algorithm selects a starting point as the coordinate with greater Y value on the region of points of X and Z within a ± 0.01 mm threshold. Then, it analyses neighbour points in order to find a discontinuity in the Y values, i.e., sudden smaller followed by higher Y values with the aim of finding the coronal suture. Once the suture region is found, the Bregma is selected as point in the region with smaller Y coordinate;

4. Dakryon (d): point located at the apex of the angle formed by the frontolacrimal suture and lacrimomaxilar suture;

5. Ektokonchion (ek): Point located on the outer edge of the orbit and the furthest possible of the maxillofrontale point;

6. Eurion (eu): Most lateral point of the neuro-cranium. Has no fixed location and varies from one individual to another and from one population to another;

7. Frontotemporale (ft): most anterior point of the temporal line, located approximately at the root of the zygomatic apophysis of the frontal bone;

8. Frontomalare Temporale (fmt): point most posterior and lateral of the frontomalar suture, in the temporal region;
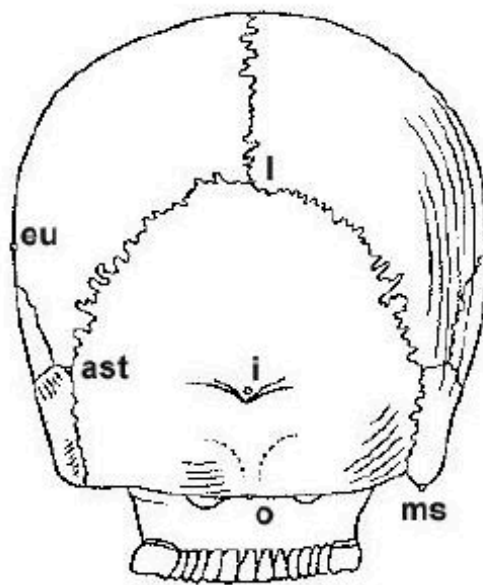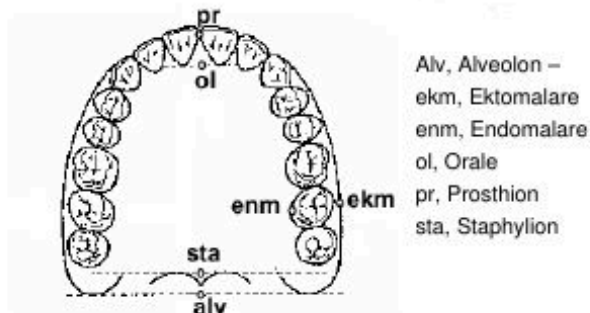
Figure 1: Skull back

9. Glabella (g): Point located just above the frontonasal suture, between the superciliary arches. Commonly is the most salient point of the front, in the sagittal plane. It may, however, constitute or form a depression, with the superciliary arch (a single continuous elevation);

10. Lambda (l): Intersection point between the sagittal and lambdoid sutures;

11. Nasion (n): Intersection point of the frontonasal suture and suture internasal. Corresponds to the root of the nose;

12. Nasoespinale (ns): Lowest point in the inferior edge of the piriform aperture at the
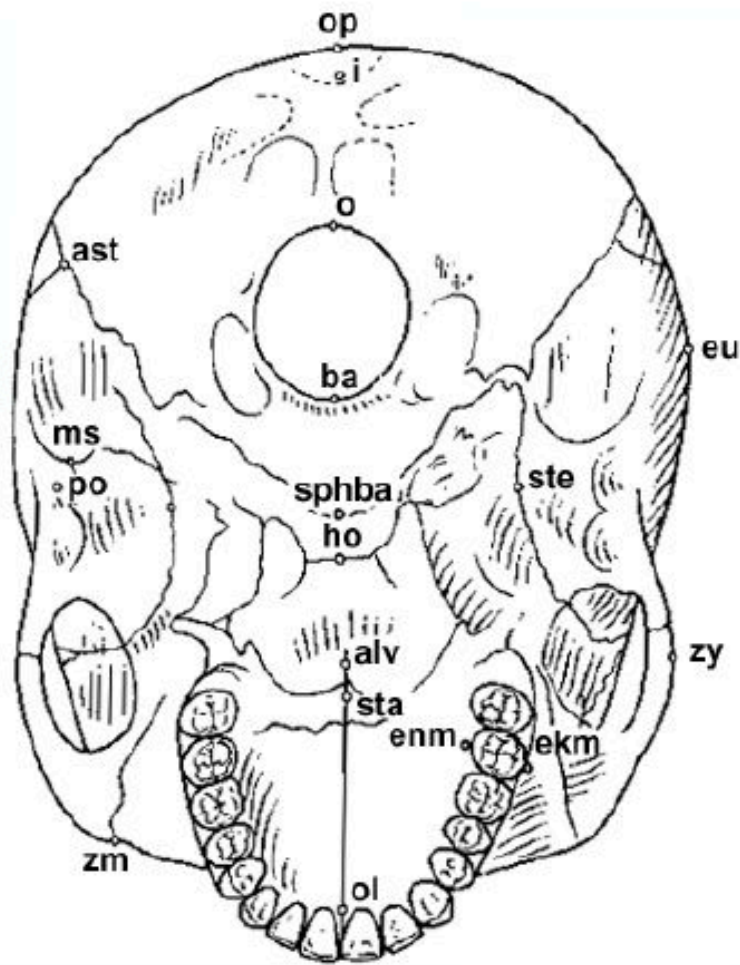
alv, Alveolon - ast, Asterion - ba, Basion - ekm, Ektomalare - enm, Endonmlare - eu, Eurion -
ho, Hormion - i, Inion - ms, Mastoideale - o, Opisthion - op, Opisthokranion - ol, Orale - po,
Porion - sphba, Sphenobasion - sta, Staphylion - ste, Stenion - zy, Zygion - zm, Zygomaxilla-
re.

Figure 2: Skull down

base of the nasal spine, designed in the Sagittal Plane. This point is called by some
authors Sub-nasale or Nasale;

13. Opisthion (o): Mid point of the posterior edge of the occipital hole;

14. Opisthokranion (op): Point more away from the glabella in sagittal plane of the occip-
ital. Sometimes coincides with the inion. There are cases where this occipital region is
more or less flat;
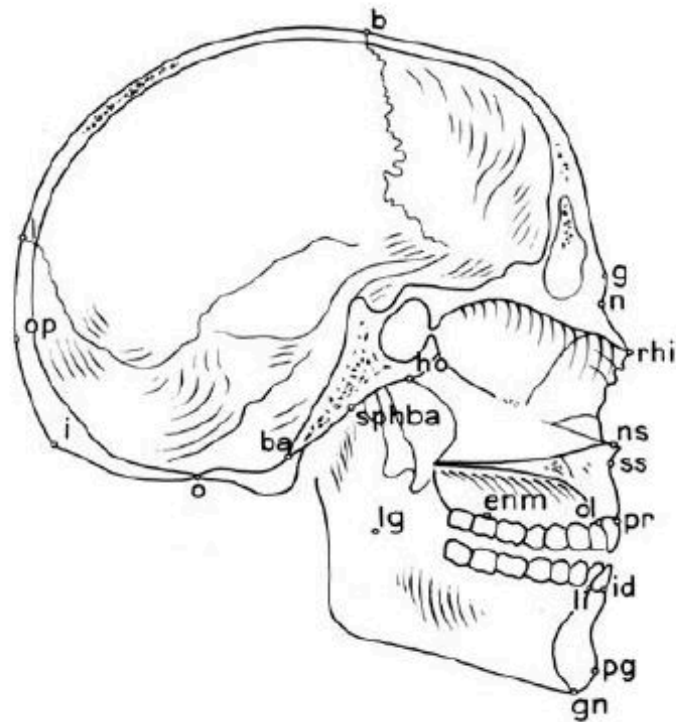
Ba, Basion – b, Bregma – enm, Endomalare – g, Glabella – gn, Gnathion – ho, Hormion – i, Inion – id, Infradentale – l, Lambda – li, Linguale – lg, Lingulare – n, Nasion – ns, Nasospinale – o, Opisthion – ol, Orale – op, Opisthokranion – pg, Pogonion – pr, Prosthion – rhi, Rhinion – spha, Sphenobasion – ss, Subspinale.

Figure 3: Skull down inside

15. Prosthion (pr): Most anterior point of the alveolar ridge between the central incisors. Corresponds to the lower end and anterior interalveolar septum in the sagittal plane;

16. Zygion (zy): most lateral point of the zygomatic arch, on each side. Given the aligned skull Zygia are defined as the points with maximum and minimum X coordinates, respectively to the right and left points. Since the zygomatic arch might not be the largest zone of the skull, we only consider the portion of the skull with negative Y values;

All illustrations representing the skull were adapted from the book of Pereira et al [48].
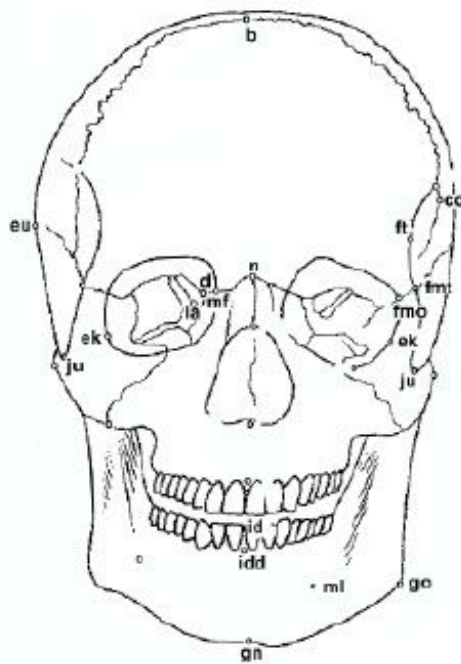
b, Bregma – co, Coronale – d, Dakyon – ek, Ektokonchion – eu, Eurion – fmo, Frontomalare orbitate- fmt, Frontomolare temporale – ft, Frontotemporale – gn, Gnathion – go, Gonion – id, Infradentale – idd, Infradentale dentale – ju, Jugale – la,Lacrimale – mf, Maxillofrontale – ml, Mentale – n, Nasion – ns, Nasospinale – or, Orbitale – prl, Prominentia laterale – pr, Prosthion – prd, Prosthion dentale – rhi, Rhionion – st, Stephanion – zy, Zygion – zm, Zygomaxillare

Figure 4: Skull front
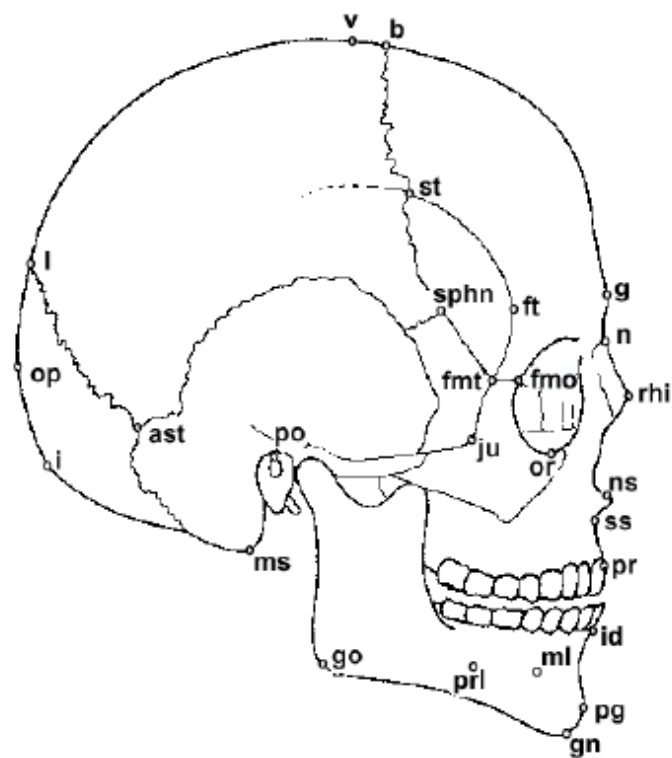
ast, Asterion – b, Bregma – fmo, Frontomalare orbitale – fmt, Frontomale temporale – ft, Frontotemporale – g, Glabella – gn, Gnathion – go, Gonion – i, Inion – id, Infradentale – ju, Jugale – l, Lambda – ms, Mastoidale – ml, Mentale – n, Nasion – ns, Nasospinale – op, Opisthokarion – or, Orbitale – pg, Pogonion – po, Porion – prl, Prominentia laterale – pr, Prosthion – rhi, Rhinion – sphn, Sphenion – st, Stephanion – ss, Subspinale – v, Vertex

Figure 5: Skull side
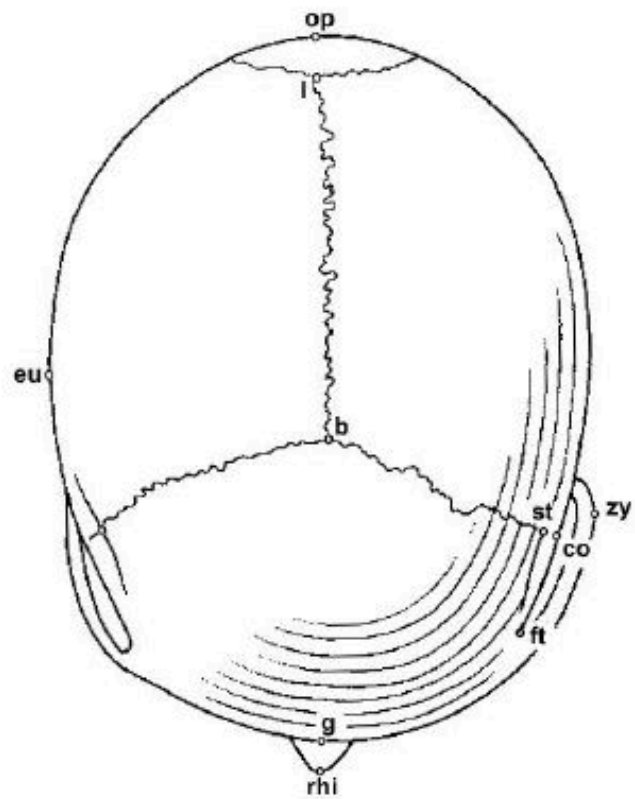
b, Bregma – co, Coronale – eu, Eurion – ft, Frontotemporale – g, Glabella – l, Lambda – op, Opisthokranion – rhi, Rhinhion – st, Stephanion – zy, Zygion

Figure 6: Skull top

Appendix B Measures

THE following measure were used by the iDryas team (credit of Catarina Coelho [49]) to classify the skulls (using the software FORDISC):

1. GOL (maximum skull length): distance (straight line) between *Glabella* and *Opisthokranion.*;

2. XCB (maximum skull width): maximum width on the sagittal plane;

3. ZYB (bizygomatic width): the distance between both *Zigyon* points;

4. BBH (*Basion-Bregma* height): distance between *Basion* and *Bregma*;

5. BNL (*Nasion-Basion* length): distance between *Basion* and *Nasion*;

6. BPL (*Basion-Prosthion* length): the distance (strait line) between *Basion* and *Prosthion*;

7. MAB (*maxillo-alveolar* width): is the maximum width of the alveolar arch on the outer surface (the distance between the two ectomalares);

8. MAL (*maxillo-alveolar* length): distance between the *Prosthion* and *Alveolon*;

9. AUB (Biauricular width): the minimum exterior width measured in the root of the zygomatic processes;

10. UFHT (superior facial height): distance between *Nasion* and *Prosthion*;

11. WFB (minimum facial width): distance between both *Fronto-Temporalle* points;

66

12. UFRR (superior facial width): distance between both *Frontomalar-Temporalle* points;

13. NLH (nasal height): distance between the *Nasion* and *Nasoespinal*;

14. NLB (nasal width): maximum width of the nasal aperture;

15. OBB (orbital width): distance between *Dakryon* and *Ektokonchion*;

16. OBH (orbital height): distance between the border of the inferior and superior orbit;

17. EKB (bi-orbital width): distance between both *Ektokonchion* points;

18. DKB (inter-orbital width): distance between both *Dacryon* points;

19. FRC (frontal line): distance, in the sagital plane, between the *Nasion* and *Bregma*;

20. PAC (parietal line): distance, in the sagital plane, between *Bregma* and *Lambda*;

21. OCC (occipital line): distance, in the sagital plane, between *Lambda* and *Opistion*;

22. FOL (length of the *Foramen Magnum*): distance between *Basion* and *Opistion*;

23. FOB (width of the *Foramen Magnum*): distance between the lateral margins of the *Foramen Magnum*, in the lateral point with biggest curvature;

24. MDH (height of the *Mastoid process*): distance, in projection, between the *Frankfurt plane* and the nadir point of the *Mastoid process*.

Appendix C Measurement Tables for All (8) Skulls

	#21				#25			
	user #1	user #2	CC	MTF	user #1	user #2	CC	MTF
ZYB	0	0	0	0	136.7	136.7	136	137
GOL	171.5	171.3	172	169	182.1	182.1	181	181
BBH	0	0	0	0	142.7	142.7	142	143
BNL	0	0	0	0	105.3	105.3	106	107
XCB	128.1	128.1	124	126	135	135	131	131
FRC	107.4	108.4	108	108	116.6	116.6	114	115
BPL	0	0	0	0	102.8	102.8	103	104
UFHT	65.5	64.6	62	65	64.9	65.6	62	64
MAB	58.9	58.9	57	59	67.6	67.3	66	65
AUB	105.1	104.9	98	98	117.2	117.8	110	108
NLH	49	48.2	46	46	48.5	48.5	47	46
UFBR	95.4	95.3	95	95	108.9	109.1	106	109

	#38				#39			
	user #1	user #2	CC	MTF	user #1	user #2	CC	MTF
ZYB	121.7	121.7	119	121	0	0	0	0
GOL	180.1	180.1	180	175	166.5	165.9	169	164
BBH	132.9	132.9	133	133	133.8	133.8	132	133
BNL	95.2	95.2	95	96	90.4	90.7	84	90
XCB	137.7	137.7	136	137	121.2	121.2	114	117
FRC	109.1	109.1	112	107	106.3	106.2	98	98
BPL	0	0	0	0	94.1	94.1	93	92
UFHT	0	0	0	0	59.5	59.7	54	56
MAB	61.8	61.9	61	61	0	0	0	0
AUB	105.4	111.5	101	101	109.7	109.3	100	98
NLH	49.8	49.9	48	47	44.2	44.3	44	44
UFBR	97.6	97.7	98	99	92.8	92.3	92	94

	#57				#65			
	user #1	user #2	CC	MTF	user #1	user #2	CC	MTF
ZYB	0	0	0	0	136.2	136.2	134	136
GOL	182.7	182.7	185	182	174.7	174.7	175	175
BBH	0	0	0	0	139.3	139.3	139	139
BNL	0	0	0	0	105.5	106.3	106	106
XCB	138.6	138.7	137	137	130.3	130.3	123	124
FRC	122.2	125.2	116	115	110.1	109.4	109	109
BPL	0	0	0	0	103.4	104.2	103	105
UFHT	59.4	55.9	57	58	62.8	63.3	56	60
MAB	61	61.2	61	61	63.5	63.6	62	64
AUB	112.9	112.1	108	109	111.8	108.8	102	99
NLH	42.7	40.2	44	44	44.7	45.4	45	44
UFBR	101.6	101.7	101	103	112.7	112.4	113	114

	#66				#67			
	user #1	user #2	CC	MTF	user #1	user #2	CC	MTF
ZYB	0	0	0	0	126.5	126.5	126	126
GOL	184.6	184.9	186	179	180.8	181.4	182	173
BBH	130	130	130	130	131.9	131.9	131	130
BNL	96.6	96.6	96	97	105.5	105.5	104	105
XCB	141.9	141.9	133	137	139.5	139.5	122	126
FRC	114.4	114.4	113	112	102.6	102.5	107	108
BPL	98.9	98.9	94	99	102.2	102.2	94	102
UFHT	59.8	59.8	57	58	68.5	68.5	64	66
MAB	61.6	61.6	60	61	61.2	61.2	61	61
AUB	124.5	125.1	123	114	115.2	115.2	107	107
NLH	42.7	42.7	44	43	48.9	49.2	49	49
UFBR	106.4	106.3	107	108	105.2	105.5	106	108

Appendix D Building the Application

The building system is based on CMake. Dependencies are minimal, requiring only a C++ compiler. The principal features are the automatic generation of the makefiles for the target platform, the *out of source* building and the support for directory hierarchies. The programmer only needs to write one text file (CMakeLists.txt) in the root of the project with the configurations needed. Optionally, each subdirectory of the project can have his own configuration file (CMakeLists.txt). The build process takes places in two stages. First, platform specific building files are created. Second, with the previous created configuration files the compilation tool(s) installed on the target platform are used to build the executable.

Listing 3 shows the contents of the CMakeLists.txt file.

```
PROJECT(CraMs)

# minimum version
cmake_minimum_required(VERSION 2.6)

# searches for VTK
IF(NOT VTK_BINARY_DIR)
FIND_PACKAGE(VTK)
IF(NOT VTK_DIR)
   MESSAGE(FATAL_ERROR "Please set VTK_DIR.")
ENDIF(NOT VTK_DIR)
INCLUDE(${VTK_USE_FILE})
ENDIF(NOT VTK_BINARY_DIR)


# -std=c++11 WILL BE IGNORED BY VISUAL STUDIO - MUST INSTALL LATEST CTP
SET(CMAKE_CXX_FLAGS "${CMAKE_CXX_FLAGS} -Wall -std=c++11")

# use what QVTK built with
SET(QT_QMAKE_EXECUTABLE ${VTK_QT_QMAKE_EXECUTABLE} CACHE FILEPATH "")
SET(QT_MOC_EXECUTABLE ${VTK_QT_MOC_EXECUTABLE} CACHE FILEPATH "")
SET(QT_UIC_EXECUTABLE ${VTK_QT_UIC_EXECUTABLE} CACHE FILEPATH "")
```

```
FIND_PACKAGE(Qt4)
IF(QT_USE_FILE)
   INCLUDE(${QT_USE_FILE})
ELSE(QT_USE_FILE)
   SET(QT_LIBRARIES     ${QT_QT_LIBRARY})
ENDIF(QT_USE_FILE)

SET (SRCS
   main.cxx Ellipsoid.cxx ModelUtils.cpp MouseKeyboardInteraction3D.cpp
      TestNormals.cpp CompareCoordinates.cpp BoxWidgetSelectCallback.cpp
      curvatures.cpp
)

# Use the include path and library for Qt that is used by VTK.
INCLUDE_DIRECTORIES(
        ${QT_INCLUDE_DIR}
        ${CMAKE_CURRENT_BINARY_DIR}
        ${CMAKE_CURRENT_SOURCE_DIR}
)

# src, inc and ui files
INCLUDE_DIRECTORIES(${VTK_TDX_INCLUDE_PATH})
QT4_WRAP_UI(UI_SRCS GUI.ui)
QT4_WRAP_CPP(MOC_SRCS GUI.h)
SET(SRCS ${SRCS} ${MOC_SRCS} GUI.cxx GUI.h)

# add executable
ADD_EXECUTABLE( skull3d MACOSX_BUNDLE ${SRCS} ${UI_SRCS})

# link libraries
TARGET_LINK_LIBRARIES( skull3d
   QVTK
   ${QT_LIBRARIES}
   vtkRendering
   vtkGraphics
   vtkIO
   vtkCommon
)
```

Listing 3: Pseudo code for the algorithm to get the point with maximum curvature, taking into account the neighbours

The configuration under GNU/Linux systems is as simple as presented on listing 4. The user only needs to execute the command:

```
$ cmake .
```

Listing 4: cmake command

followed by:

```
$ make
```

Listing 5: make command

The output of the configuration process is the following:

```
[user@host crams]$ cmake .
-- The C compiler identification is GNU 4.7.2
-- The CXX compiler identification is GNU 4.7.2
-- Check for working C compiler: /usr/lib64/ccache/cc
-- Check for working C compiler: /usr/lib64/ccache/cc -- works
-- Detecting C compiler ABI info
-- Detecting C compiler ABI info - done
-- Check for working CXX compiler: /usr/lib64/ccache/c++
-- Check for working CXX compiler: /usr/lib64/ccache/c++ -- works
-- Detecting CXX compiler ABI info
-- Detecting CXX compiler ABI info - done
-- Looking for Q_WS_X11
-- Looking for Q_WS_X11 - found
-- Looking for Q_WS_WIN
-- Looking for Q_WS_WIN - not found
-- Looking for Q_WS_QWS
-- Looking for Q_WS_QWS - not found
-- Looking for Q_WS_MAC
-- Looking for Q_WS_MAC - not found
-- Found Qt4: /usr/bin/qmake-qt4 (found version "4.8.4")
-- Configuring done
-- Generating done
```

Listing 6: Running CMake under GNU/Linux systems

Under Windows, the user may use the application CMake (has a nice GUI) to generate the configuration files, as depicted on figure 7.

After the configuration is done, the project can be easily loaded into Visual Studio to compile and/or further develop stages, as depicted by figure 8.
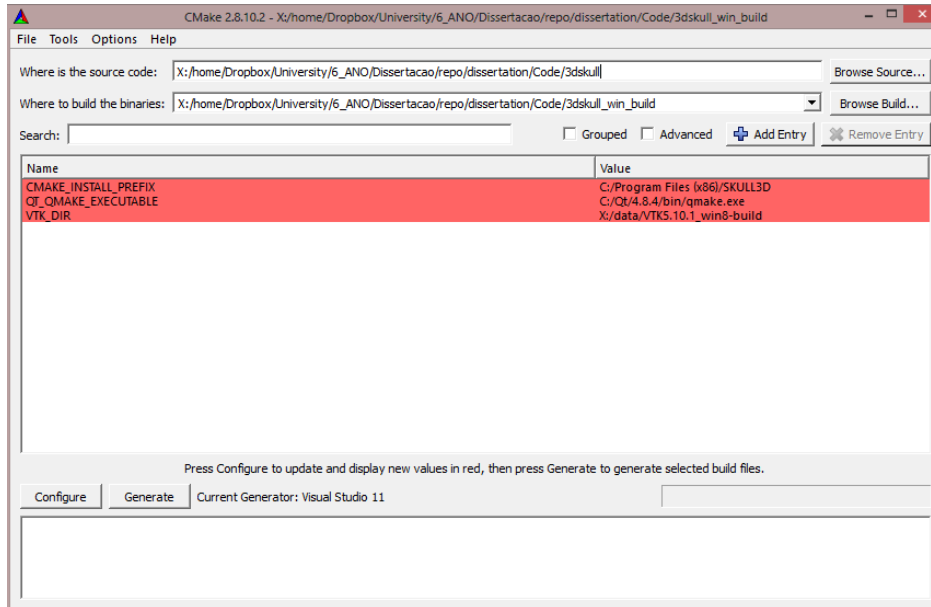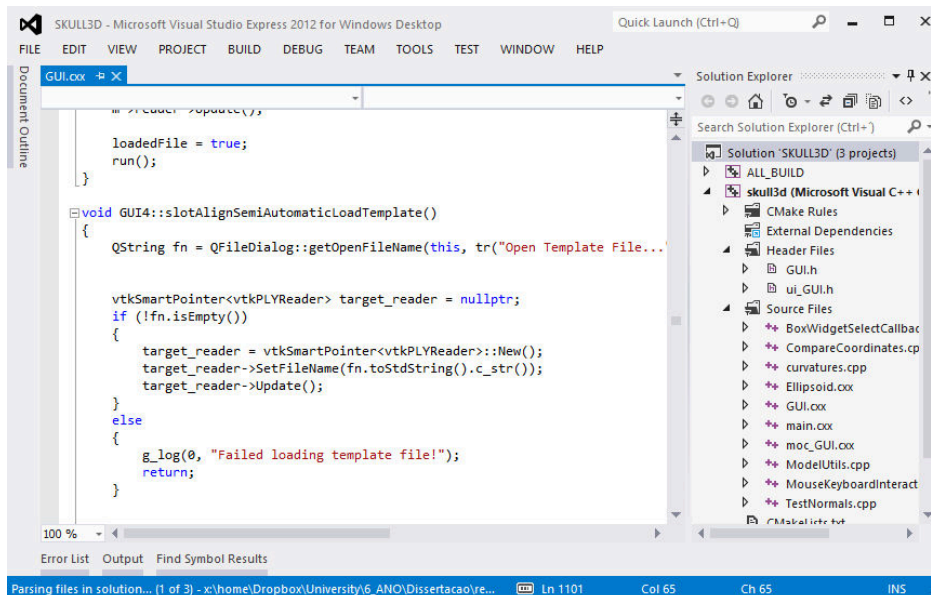
Figure 7: CMake GUI configuration tool on Windows

Figure 8: The project loaded into Visual Studio (2012)